THESIS FOR THE DEGREE OF DOCTOR OF PHILOSOPHY

Additive-Driven Improvements in Interfacial Properties and Processing of Thermomechanical Pulp-Polymer Composites

Seyedehsan Hosseini

Department of Chemistry and Chemical Engineering

CHALMERS UNIVERSITY OF TECHNOLOGY

Gothenburg, Sweden 2023

Additive-Driven Improvements in Interfacial Properties and Processing of TMP-Polymer Composites

Seyedehsan Hosseini
ISBN 978-91-7905-940-8

Doktorsavhandlingar vid Chalmers tekniska högskola
Ny serie nr 5406
ISSN 0346-718X

Department of Chemistry and Chemical Engineering
Chalmers University of Technology
SE-412 96 Gothenburg
Sweden
Telephone + 46 (0)31-772 1000

Cover:
The cover photo shows "Svartedalen Naturreservat" in northern Gothenburg area captured by me.

Printed by Chalmers Digitaltryck

Gothenburg, Sweden 2023

Additive-Driven Improvements in Interfacial Properties and Processing of TMP-Polymer Composites

Seyedehsan Hosseini
Department of Chemistry and Chemical Engineering
CHALMERS UNIVERSITY OF TECHNOLOGY

Abstract

Efforts to address environmental concerns have resulted in new regulations designed to plan the reduction of plastic and synthetic polymer usage, necessitating the search for sustainable natural alternatives with comparable cost-effectiveness and mechanical performance. Thermomechanical pulp (TMP) fibres are one of the most affordable natural fibres that have no chemical refining in production, production have a high yield of 90-98% and TMP fibres have been demonstrated to improve the mechanical characteristics (strength, stiffness and toughness) of wood-polymer composites (WPCs) compared to the pure polymer. The integration of TMP fibres with non-polar synthetic polymers remains a challenge due to surface polarity differences. This PhD thesis aims to ease the processing of TMP fibre composites through the incorporation of additives. The hypothesis posits that incorporating magnesium stearate (MgSt), molybdenum disulfide (MoS_2) and alkyl ketene dimer (AKD) as additives in TMP composites will enhance interfacial properties, resulting in improved processability and flow behaviour at high temperatures. MoS_2 is known for its interaction with lignin, which exists in TMP and MgSt is recognised for its ability to improve flow in pharmaceutical processing when combined with cellulose, also a component of TMP. AKD modifies the hydrophilic properties of lignocellulosic surfaces.

The experimental work explores the effect of these additives on the properties of TMP composites of ethylene acrylic acid copolymer (EAA) and polypropylene (PP) matrices. The dynamic mechanical analysis (DMA) and mechanical analysis results reveal that MoS_2 exhibits superior interaction with TMP fibres, yielding enhanced interfacial properties compared to MgSt in between EAA and TMP fibres. Rheological studies elucidate the transition from a fluid-like state to a network-like structure upon the incorporation of TMP into the PP matrix. The incorporation of AKD with C18 reduces the viscosity of TMP-PP composites and PP itself, and, as determined through theoretical Hansen solubility parameter (HSP) calculations, increases compatibility between cellulose in TMP fibres and PP. The addition of AKD influences both the colour (lighter) and shape (smoother surface) of the extrudate filaments in the TMP-PP composites, indicative of improved processing. In addition, frictional analysis demonstrates the reduction of the coefficient of friction (COF) between metal and TMP fibre by MgSt and AKD treatments.

Keywords: thermomechanical pulp, alkyl ketene dimer, molybdenum disulfide, magnesium stearate, rheology, friction.

“Assume Formlessness: Everything changes. What worked today won’t necessarily work tomorrow. And you must adapt to thrive.”

Robert Greene

LIST OF PAPERS

1. **Molybdenum desulphated—A traditional external lubricant that shows interesting interphase properties in pulp-based composites**

   Seyedehsan Hosseini, Abhijit Venkatesh, Natal Boldizar, Gunnar Westman

   Polymer Composites, Volume 42, Issue 9, September 2021 Pages 4884-4896

   https://doi.org/10.1002/pc.26197

2. **Alkyl ketene dimer modification of thermomechanical pulp promotes processability with polypropylene**

   Seyedehsan Hosseini, Robin Nilsson, Anna Ström, Anette Larsson and Gunnar Westman

   Polymer Composites, October 2023.

   https://doi.org/10.1002/pc.27818

3. **Reducing friction between metal and thermo-mechanical pulp using alkyl ketene dimers and magnesium stearate**

   Seyedehsan Hosseini, Roujin Ghaffari, Anette Larsson, Gunnar Westman, and Anna Ström

   Submitted

CONTRIBUTION REPORT

1. Shared main author. I planned the experiments and performed sample preparation, thermal analysis, FTIR, EDX and SEM studies and part of the mechanical testing. The sample preparation for SEM and DMA was mainly performed by Abhijit Venkatesh. I wrote the manuscript with Abhijit Venkatesh and input from the other co-authors.
2. Main author. Responsible for planning and performing the majority of the synthesis and experimental characterisation. Wrote the first draft of the manuscript, reviewed and edited the article with the help of my supervisors.
3. Main author. Responsible for initial design of the study, performed all experimental characterisation except IR microscopy. Evaluation together with co-authors. Wrote the first manuscript draft, reviewed and edited the article aided by my supervisors.

ABBREVIATIONS

AKD	Alkyl ketene dimer
ATR-FTIR	Attenuated total reflectance-Fourier transform infrared spectroscopy
COF	Coefficient of friction
DSC	Differential scanning calorimetry
DMA	Dynamic mechanical analysis
EAA	Ethylene acrylic acid copolymer
EDX	Energy-dispersive X-ray spectroscopy
ETC	Environmental test chamber
HSP	Hansen's solubility parameters
MCC	Microcrystalline cellulose
MgSt	Magnesium stearate
MoS_2	Molybdenum disulfide
NMR	Nuclear magnetic resonance spectroscopy
OH	Hydroxyl
PP	Polypropylene
SEM	Scanning electron microscopy
TGA	Thermogravimetric analysis
TMP	Thermomechanical pulp
WPCs	Wood-polymer composites
Xc	Degree of crystallinity

Table of Contents

1. Introduction

Efforts to mitigate environmental concerns have led to the implementation of new regulations aims at planning the reduction in the use of plastic and synthetic polymers in both industrial and daily life applications.[1,2] The primary challenge in this endeavour is finding a suitable substitute that is derived from sustainable natural sources and which possesses similar qualities in terms of cost-effectiveness, processability and mechanical performance (strength, stiffness, toughness and elasticity) when compared to the prevalent synthetic polymers.

Sweden, occupying a mere fraction of 1% of the world's forested lands, is a leading global exporter of pulp, paper and sawn timber products. The total land area of Sweden is 40.8 million hectares, with 22.5 million hectares constituting productive forest lands.[3] The rate of forest growth has exceeded the rate of deforestation, consistently throughout the 20th century and beyond.[3] The utilisation of natural fibres derived from trees is a viable alternative for synthetic polymers and plastics to be considered. Sawdust and thermomechanical pulp (TMP) fibres, derived from the forest, are among the most cost-effective materials currently available and have the potential to be price-competitive with synthetic plastics. Wood-polymer composites (WPCs), consisting of wood and polymer, have been commercially available in small quantities since the 1960s[4] and are typically reinforced with sawdust or wood powder.[5] Wood powder, commonly utilised as fillers, lack the reinforcement properties of fibres.[5] In contrast, TMP fibres have been demonstrated to enhance the mechanical characteristics of WPCs.[6] The application of TMP fibres in WPCs with a wide range of fibre content (30 wt% or lower,[6] 50 wt%[7,8] and 60 wt%[9]) has been studied. However, in almost all studies, fibre entanglement during processing has emerged as a significant challenge. Additionally, excessively high wood fibre loadings results in agglomeration during melt processing.[10,11]

The achievement of optimal composite (processability and mechanical properties) properties is contingent upon the compatibility of the matrix and filler, as well as the quality of the interface between them. The main challenge in the wood fibre-polyolefin system lies in the integration of the relatively polar lignocellulosic surface of TMP with a typically non-polar synthetic polymer.

This PhD thesis aims to investigate the effect of different additives for improved processing of TMP fibre composites. These composites can have versatile applications, including but not limited to kitchen utensils, interior car design manufacturing and packaging materials, plus

crates and pallets. The hypothesis of this study postulates that the incorporation of different additives, magnesium stearate (MgSt), molybdenum disulfide (MoS_2) and alkyl ketene dimer (AKD) as additives in TMP composites will result in improving interfacial properties between the fibres and the matrix material and as a result improves processability and flow behaviour of the composites.

MoS_2 was used as the external lubricant due to its ability to interact with the aromatic structure in lignin,[12,13] while MgSt was chosen as the internal lubricant as it is a commonly employed lubricant during the manufacturing process of compressed pharmaceutical dosage forms.[14,15]

The application of sizing agents, a chemical compound used to reduce the penetration of water or other liquids into the paper, is a widely adopted method in the pulp and paper industry. AKDs are commonly used as sizing agents[16,17] and possess a dual polarity, a polar component that could interact with the cellulose surface and a non-polar hydrophobic component that could be compatible with polyolefins. While prior research, such as the study by Quillin *et al*.[18], has explored the influence of AKD modification on bleached kraft cellulose pulp in composites with polypropylene (PP), which indicated improved cellulose dispersibility within the matrix, none of these studies have specifically investigated the processing of TMP and PP, particularly in the context of extrusion.

It is believed that the decrease in surface defects at elevated extrusion rates and shear rates is associated with an increased wall slip[19]. This slip velocity, in turn, is linked to the shear stress at the wall of the extruder through the coefficient of friction (COF)[20]. Marton[21] has studied the impact of AKD on metal-paper friction and the results from this study show that AKD reduces the friction between metal and paper surfaces. In addition, previous research has provided evidence suggesting that unbound AKD molecules contribute to the reduction of friction between paper surfaces.[22,23] These unbound AKD molecules are believed to play a crucial role in decreasing the friction encountered in paper. Furthermore, studies have indicated that AKD molecules with longer side chains exhibit greater effectiveness in reducing paper friction compared to those with shorter side chains.[22]

In Paper I the TMP fibres were reinforced with ethylene acrylic acid copolymer (EAA) copolymer as a matrix, with MoS_2 and MgSt used as lubricants and additives to improve the processability and compatibility of the TMP fibres with the matrix. In Paper II, PP was used as a matrix and the TMP fibres were modified with AKD to enhance their compatibility with the matrix during the extrusion process. Paper III examined the influence of AKD and MgSt on

the friction between metal and TMP at varying temperatures. In summary, the present study aims to investigate the following set of hypotheses:

1. The incorporation of MgSt, MoS_2 and AKD as additives in TMP composites will positively impact the interfacial properties between the fibres and the matrix material, leading to improved processability and flow behaviour (Paper I and II).

2. Treatment of TMP fibres with AKD and MgSt lead to a reduction in the COF between metal and fibres (Paper III).

1.1 Aim

This PhD thesis aims to gain a comprehensive understanding of the surface properties, frictional and flow properties of TMP composites. The research is focused on investigating the effect of additives, MgSt and MoS_2, on the interfacial properties and mechanical properties of TMP composites. Additionally, the effect of modification of TMP with AKD addition on the processability and flow behaviour of the composites is explored. The impact of AKD and MgSt treatment on the frictional behaviour of TMP fibres is also examined. This research aims to contribute to the advancement of knowledge in the field of TMP composites and to provide valuable insights to help improve the processing of high wt% TMP composites.

2 Background

2.1 Thermomechanical pulp (TMP)

TMP is a type of pulp produced by processing wood chips using heat and mechanical refining. The yield of TMP from wood chips is high (90 and 98%).[24] The mechanical refining process is used to separate fibre bundles and increase the surface area of the fibres by fibrillation of the cell wall structures.[25] TMP is comprised of roughly 40% cellulose, 30% hemicellulose and 30% lignin.[26]

The TMP fibres are composed of different layers, with the outer walls mostly comprising lignin, hemicelluloses and a small amount of cellulose microfibrils that form an irregular network structure. The inner layers of the TMP fibres consist mainly of cellulose, which is mostly located in the secondary cell wall layers; these have a homogeneous fibrillar structure.[27,28]

2.1.1 Cellulose

Cellulose, the primary component of plant fibres, plays a crucial role in providing mechanical strength to plants. It is composed of chains organised through hydrogen bonds and hydrophobic interactions.[29] Scientists have identified four major types of cellulose allomorphs, namely Cellulose I, II, III and IV, based on their distinctive X-ray diffraction patterns. Among these, Cellulose I is the most abundant, existing in both α and β forms, with the β form being extensively studied.[29] Cellulose adopts a microcrystalline structure, featuring both crystalline and amorphous regions. These distinct regions contribute to the mechanical properties of the plant cell wall.[30] The various structural levels of a plant cell wall are shown schematically in Figure 1.

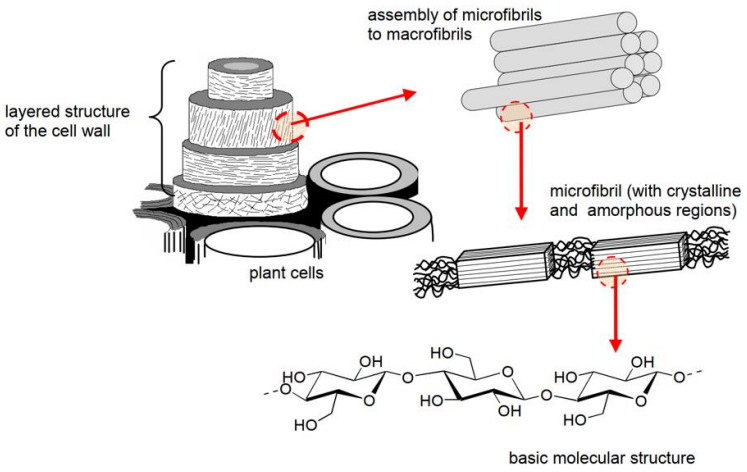

Figure 1. Schematic diagram of the different structural levels of cellulose (reproduced with permission from the PhD thesis of M. Hassani).[26]

2.1.2 Lignin

Lignin is a complex macromolecule found in the support tissues of vascular plants and some algae. It servs as the adhesive that holds the fibres together. For softwood, the amount of lignin varies between 26-32 %, whilst for hardwood it varies between 20-26 %[31] and is located on the surface of the fibre.[26] Lignin has both aliphatic and aromatic structures[32] and a lower mechanical strength compared to cellulose.[6] It plays a crucial role in the structure of plant cell walls and is the second most abundant biopolymer in the world after cellulose.[31]

2.2 Wood-based composites

2.2.1 Polymers for pulp fibre composites

Polymers can be classified as either thermoplastics or thermosets. Thermoplastics, such as polyethylene, polystyrene, polyvinyl chloride and PP, are amorphous or semi-crystalline and soften continuously as the temperature increases.[33] By Contrast, thermosets, such as vinyl esters, phenol formaldehyde, polyester and epoxy resin, polymerise and stiffen as temperature increases, with regular molecular chain arrangements and strong intermolecular bonds.[34] Compared to thermosets, thermoplastics are more economically feasible, have a quicker processing route and are recyclable, making them more commonly used in wood fibre composites.[35] For use in wood-based composites, thermoplastic polymers must have a lower softening temperature than the thermal degradation of the wood components. The interface

between the polymer and the pulp plays a crucial role in transforming the properties of the fibre and vice versa. [35–37]

EAA copolymer is a favourable candidate for use in natural fibre composites due to its low processing temperature (150-200 °C), which reduces the risk of thermal degradation of the cellulose fibres.[38] Additionally, EAA, see Figure 2a, has carboxylic functional groups on its surface, making it more hydrophilic compared to PP (see Figure 2b) and potentially compatible with TMP. On the other hand, PP exhibits a range of advantageous properties and is cost-effective, which contributes to its widespread utilisation across various industries.[39] One of the major advantages of PP lies in its high degree of temperature resistance, rendering PP particularly suitable for diverse applications.[40] Amongst other things, PP finds applications in household items, labelling, packaging and textiles.[41]

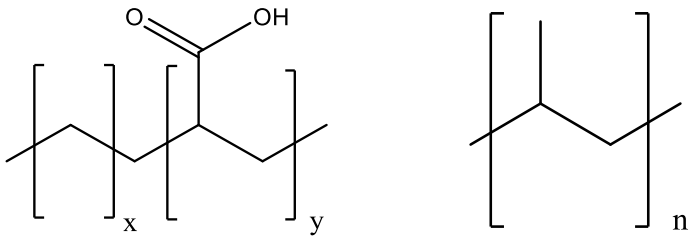

a b

Figure 2. Structures of (a) EAA copolymer and (b) PP.

2.3 TMP-polymer interface and the effects of modification

The interface between the matrix and filler is crucial in determining the properties of composite materials. Weak fibre-matrix interfacial bonding, resulting from low compatibility, can lead to inferior mechanical properties and reduced processability in wood fibre composites.[42] This is often manifested through debonding, which hinders the load transfer between the fibre and matrix.[43]

To enhance the compatibility between matrix and fibres in wood fibre composites, both matrix resin modification and fibre surface treatment have been explored.[44,45] Effective interfacial coupling necessitates a coupling agent with a hydrophilic group that can chemically react with the functional groups on the fibre surface and a hydrophobic group compatible with the polymer matrix, thus improving fibre-matrix compatibility.[42]

The TMP used in composites consists of lignin, hemicellulose and cellulose. These contain numerous polar hydroxyl and phenolic hydroxyl functional groups, resulting in a chemically polar surface and, consequently, a poor fibre-matrix interface.

Two main methods for enhancing the TMP fibre-matrix interface have been identified in the literature: physical modification using additives and lubricants and chemical modification. Internal lubricants with polar groups, such as carboxylic and amine groups, interact with the hydroxyl groups of fibres, whereas external lubricants, typically lacking polar chemical groups, reduce friction between the composite and metal surfaces or between fibres and the matrix.[46]

Lee *et al.*[47] have investigated various physical compatibilisers and additives, such as phenol formaldehyde and urea formaldehyde, to improve the interface characteristics of TMP fibres and PP. Not only does using these additives enhance compatibility, it also improves tensile strength.

MoS_2 and MgSt are two potential additives for improving the compatibility between TMP fibres and the matrix. MoS_2's interaction with the aromatic structure in lignin suggests it may further improve compatibility between TMP fibres and the matrix.[12] Moreover, tribological tests revealed that the addition of MoS_2 reduces friction and wear in steel industry.[13] MgSt is another additive that has shown potential for increasing the fluidity of microcrystalline cellulose (MCC).[48,49]

Chemical modification of fibres aims to alter their chemical structure, improving compatibility with the matrix and providing better properties in various applications. The most common chemical modifications are etherification, esterification and oxidation. Etherification introduces ether groups into the cellulose chain, improving solubility and reactivity. Esterification substitutes hydroxyl groups with ester groups, increasing stability and hydrophobicity. Oxidation introduces oxygen into the cellulose chain, increasing hydrophilicity and reactivity.[26,50]

Rozman *et al.*[51] studied the modification of TMP with silane and its impact on the properties of TMP-urea formaldehyde composite in compression moulding. They found that the silane system improved the modulus of elasticity of the composite compared to unmodified TMP. Additionally, maleated PP was considered as an alternative to PP, as it has been shown to react with cellulose.[50] However, no reaction was found between TMP and maleated PP, suggesting that the lignin in TMP fibres impedes the reaction.[52–54]

Incorporating maleic anhydride and benzoyl peroxide as chemical coupling agents has been studied. The aim was to enhance the interfacial properties between TMP fibres and PP by making a bridge between the two components. The addition of these agents reduced fibre pullouts during mechanical failure, indicating improved compatibility between TMP fibres and PP.[55] The reduction in fibre pullouts is an indicator of improved compatibility between TMP fibres and PP. Similarly, evaluating benzoylated and lauroylated TMP fibres-PP interfacial properties showed improved compatibility between TMP fibres and PP.[56]

Esterification is a widely used method for modifying the surface of TMP fibres to decrease hydrophilicity and enhance thermal properties (improving the ability to withstand higher temperatures), enabling the development of composites in the future.[57] AKD is a commonly used chemical for modifying pulp fibres and is widely used in the pulp and paper industry for hydrophobizing fibre surfaces.[58] The reaction between AKD and the cellulose in the fibres is thought to result in the formation of a beta-keto ester bond, which replaces the hydroxyl (OH) groups and increases the hydrophobicity of the fibres.[58] A schematic diagram of the reaction between AKD and cellulose is shown in Figure 3.

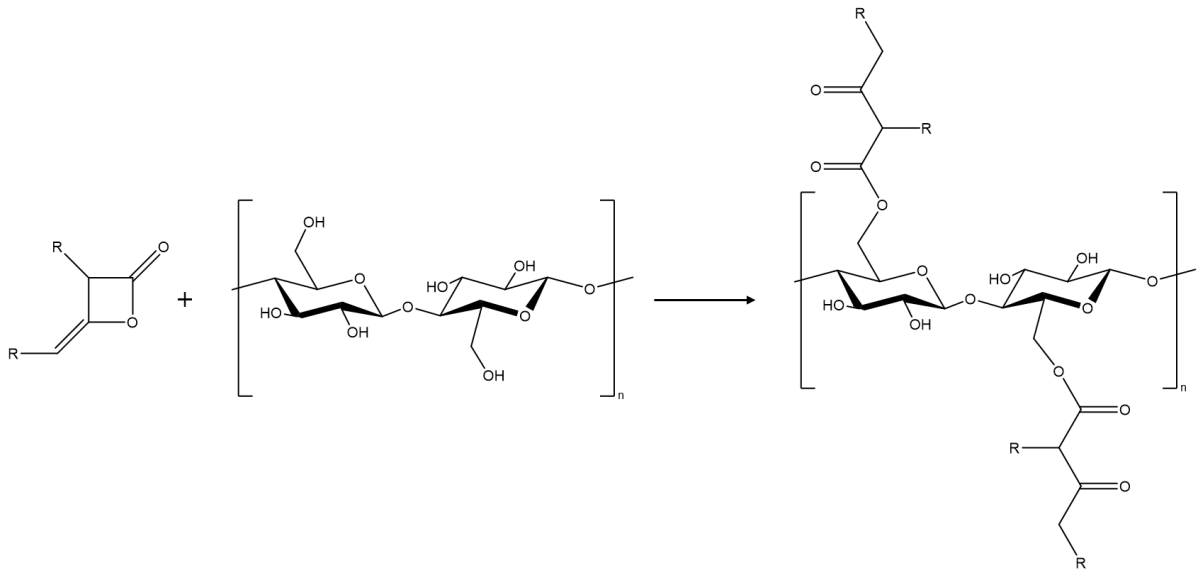

Figure 3. Schematic diagram of the AKD and cellulose reaction.

2.4 Tribology of natural fibres, friction and flow behaviour

Tribology, which involves the study of friction, lubrication and wear, has traditionally been applied to the examination of contact surfaces in various systems, such as machine components and bearings.[59] To gain insight into the tribological properties of natural fibres, various tribological measurements have been used, including the pin-on-disk,[60–62] sliding tester[63] and horizontal-plane principle.[22] The goal of these studies was to evaluate how natural fibres, such as kenaf fibre,[64–66] jute fibre[67–69] and hemp fibre,[70] affect the wear and frictional properties of composites. However, the studies did not focus on the coefficient of friction between TMP and metal at temperatures relevant to thermal processing. In a study[71] conducted by Svensson *et al.*, the research explored the COF between spruce wood chips (the source of TMP fibres) and stainless steel. This investigation encompassed a temperature spectrum ranging from 100 to 180 °C. The outcomes of this investigation elucidate a discernible pattern, wherein the COF demonstrates its apex at around 165 °C, followed by a decline.

A critical aspect affecting the quality of extruded WPCs is their visual appearance and the absence of surface imperfections, which manifest as an uneven and rough surface texture in the extrudate. These surface defects in WPCs tend to decrease when operating at high extrusion rates[72] and high shear rates.[73] It is believed that both of these factors contribute to an increased occurrence of wall slip or enhanced slip velocity between the extruder/die system and the WPC material. This slip velocity, in turn, has a direct correlation with the shear stress at the extruder's wall or die ($\sigma_{\text{wall stress}}$), which is governed by the COF, as described by Equation 1.

$$\sigma_{\text{wall stress}} = \text{COF} * V_w \quad (1)$$

where V_w is the slip velocity.[20]

2.4.1 Effect of AKD and MgSt on frictional properties

Marton[21] has studied the use of long-chain alkyl fatty acid ester of cellulose and AKD ketone in envelope paper. The research findings indicate that the AKD ketone contributes to reducing the friction coefficient in paper-to-paper tests. Extraction of the AKD ketone through chloroform removal increased both static and kinetic friction coefficients by 35-50% in this particular friction mode. However, the removal of AKD ketone did not significantly affect the friction coefficients in paper-to-polished metal tests. The article concludes that adding AKD ketone can lead to decreased friction, particularly in paper-to-paper interactions.

AKD has also been shown to decrease friction properties in paper production. The unbound AKD is believed to be responsible for the reduced friction in paper. Studies have reported that AKD molecules with longer side chains are more effective in reducing paper friction than those with shorter side chains.[22]

MgSt, which has been used as an external lubricant in pharmaceutical formulations.[74] Some research efforts have been dedicated to exploring the distribution patterns of MgSt as a lubricant on the surfaces of lubricated particles, three primary possibilities have been identified, (1) formation of a monomolecular film; (2) formation of a monoparticulate layer; and (3) mono- or multiparticulate filling of superficial cavities.[75]

3 Materials & Methods

3.1 Materials

The TMP fibres utilised in the study were obtained from StoraEnso Hyltebruk, Sweden and were derived from Norway spruce (*Picea abies*). The fibre analysis of the TMP was performed using a Kajaani FS300 fibre analyser and resulted in an average fibre length and width of 3.2 mm and 35 μm, with fines content of 33%. The EAA copolymer was supplied by BIM Kemi AB, Sweden. MoS_2 and MgSt were obtained from Sigma Aldrich, Germany, with MoS_2 having a density of 5.06 g/ml and particle size < 2 μm, while MgSt had a density of 1.026 g/cm^3. The fatty acyl chlorides (hexanoyl chloride, lauroyl chloride and stearoyl chloride) were purchased from Sigma Aldrich, Germany. The PP used in the study had a melt flow rate (MFR) of 100 g/min, density of 0.902 g/mL and melting point of 160°C. The solvents used, including butyl acetate, diethyl ether, ethylene glycol, polyethylene glycol and formamide, were all obtained from Sigma Aldrich, Germany. The commercial AKD wax utilised, AQUAPEL 291-EU, in the study was kindly provided by Solenis Sweden AB and had a C18 alkyl chain length (as stated by the supplier).

3.2 Synthesis of AKD molecules, modification of TMP fibres and production of the sheets and the composites

3.2.1 TMP – EAA composites

The TMP fibres, EAA dispersion and an additive (either MgSt or MoS_2) were combined in varying proportions to achieve the desired weight fractions of dried composites, as indicated in Table 1. Compression moulding was the method of choice for the initial study, with further details of the process conditions outlined in Paper I.[76]

Table 1. The samples with their designated compositions of TMP, additive and EAA.

Sample designation	Pulp (wt%)	Additive (wt%)	EAA (wt%)
TMP	100	0	0
EAA	0	0	100
EAA-MoS_2	0	0.5	99.5
		1.5	98.5
		5	95
TMP30	30	0	70
TMP50	50	0	50
TMP70	70	0	30
TMP30-MgSt	30	1.5	68.5
TMP30-5MgSt		5	65
TMP50-MgSt	50	2.5	47.5
TMP70-MgSt	70	3.5	26.5
TMP30-MoS_2	30	1.5	68.5
TMP30-5MoS_2		5	65
TMP50-MoS_2	50	2.5	47.5
TMP70-MoS_2	70	3.5	26.5
EAA-TMP30-MgS+MoS_2	30	0.75+0.75	68.5
EAA-TMP30-5(MgSt+MoS_2)		2.5+2.5	65
EAA-TMP50-MgSt+MoS_2	50	1.25+1.25	47.5

3.2.2 Synthesising AKD from fatty acyl chlorides

Triethylamine and a fatty acid chloride (stearoyl chloride, lauryl chloride, or hexanoyl chloride) were used as reactants in this process. The reaction was conducted in butyl acetate as the solvent.

To initiate the synthesis, a stoichiometric amount of the chosen fatty acid chloride was dissolved in butyl acetate. Triethylamine was simultaneously dissolved in butyl acetate in a separate container. The fatty acid chloride solution was then gradually added to the triethylamine solution in a round-bottomed flask whilst stirring. The reaction took place at a controlled temperature of 45°C and was allowed to proceed for two hours. The mixture was continuously stirred throughout this period.

After completion of the reaction, the resulting AKD product was separated from the salt by filtration, with diethyl ether as the extracting agent. The remaining solution was subsequently evaporated using a rotary evaporator to concentrate the AKD. The AKDs obtained from hexanoyl chloride, lauryl chloride and stearoyl chloride were AKD Hex, AKD Lau and AKD St respectively. See Paper II for more details.

3.2.3 Chemical modification of TMP fibres with AKD

In Paper II, a chemical modification process was used to treat the TMP fibres with AKD.

The procedure consisted of the following steps:

- TMP fibres were initially soaked in deionised water for 30 minutes. They were then filtered and evenly spread out on aluminium foil.
- (1 g AKD Hex, 1.25 g AKD Lau, and 1.5 g AKD St) were dissolved in 50 ml ethanol and then sprayed onto 10 g of TMP fibres.
- The modified TMP fibres were then subjected to thermal treatment in an oven, held at 90°C for two hours.
- Following the thermal treatment, the TMP fibres underwent a washing process using 40°C ethanol and deionized water.
- Finally, the treated TMP fibres were allowed to air dry in a fume hood for a period of 1 day prior to their intended use.

3.2.4 Adding commercial AKD to TMP fibres

In Paper III, different proportions (0.5 wt%, 2 wt% and 5 wt%) of AKD, AQUAPEL 291-EU and MgSt were dissolved in a mixture of ethanol and diethyl ether (40/60 wt%) and then sprayed onto the paper sheets. The fibres were allowed to air dry in a fume hood for one day prior to use. Table 2 shows the list of the samples.

Table 2. Name, additive and weight-determined percentage of additive to total mass of samples used throughout the study.

Sample	Additive	wt%
TMP	None	0
TMP AKD0.5	AKD	0.5
TMP AKD2	AKD	2
TMP AKD5	AKD	5
TMP MgSt0.5	MgSt	0.5
TMP MgSt2	MgSt	2
TMP MgSt5	MgSt	5

3.2.5 Production of paper sheets

The unmodified and sprayed TMP fibres were mixed in a 1L solution of deionised water and agitated for 60,000 revolutions in an L&W pulp disintegrator at 2,900 rpm. The sheets were then made according to the TAPPI T 205 method,[77] air-dried for a week and pressed under a 345 kPa press for one day to obtain a smooth surface area.

3.2.6 Compounding modified and unmodified TMP fibres with PP

The TMP and PP were compounded to produce the composites, which were then extruded using a Haake Minilab 3 Micro Compounder. The extruded material was melted in a hot press at 190°C, at a pressure of five tons for five minutes and 10 tons for another five minutes. The material was then cooled to room temperature and cut into bars of 4 mm × 1 mm × 40 mm (width, thickness and length).

Table 3. The TMP-PP samples with their designated weight percentages of TMP fibre, AKD and PP.

Sample designation	TMP (wt%)	AKD (wt%)	PP (wt%)	AKD/TMP (wt%)
PP	0	0	100	---
PP-TMP	50	0	50	0
PP-TMP AKD Hex	50	10	40	20
PP-TMP AKD Lau	50	12.5	37.5	25
PP-TMP AKD St	50	15	35	30

3.2.7 Predicting substance compatibility, HSP analysis

Hansen's solubility parameters (HSP) offer valuable insights into the solubility characteristics of a liquid and correspond to the total energy required for vaporisation.[78] These parameters consist of three distinct components: dispersion forces (δ_D), polar cohesive energy (δ_P) and hydrogen bonding (δ_H). The total Hansen solubility parameter squared (δ_{tot}^2) is calculated as the sum of the squares of each solubility parameter and represents the total cohesive energy (E) divided by the molar volume (V). The equation for calculation is as follows:

$$\delta_{tot}^2 = {\delta_D}^2 + {\delta_P}^2 + {\delta_H}^2 \quad (2)$$

The HSP was calculated according to the group contribution method of Hoftyzer and van Krevelen,[79] Equations 3-5.

$$\delta_D = \frac{\sum n_i F_{di}}{\sum n_i V_{Fi}} \quad (3)$$

$$\delta_P = \frac{\sqrt{\sum n_i {F^2}_{pi}}}{\sum n_i V_{Fi}} \quad (4)$$

$$\delta_H = \sqrt{\frac{\sum n_i E_{hi}}{\sum n_i V_{Fi}}} \quad (5)$$

where F_{di}, F_{pi} and E_{hi} are dispersion forces, polar forces and hydrogen bond energies for each type of chemical group, taken from table values of Hoftyzer and van Krevelen.[79] n_i is the number of chemical groups of each type and V_{Fi} is the Fedor's molar volume of each group.

Equation 6[78] presents a practical approach for comparing the HSP of two materials. Using this equation, we can determine the distance (Ra) between the materials, which is contingent on their respective partial solubility parameter components. When the Ra value is small, it signifies a high degree of similarity in terms of the materials' solubility parameters. Conversely, a large Ra value indicates significant dissimilarity between the materials' solubility properties.

$$(Ra)^2 = 4(\delta_{d2} - \delta_{d1})^2 + \left(\delta_{p2} - \delta_{p1}\right)^2 + (\delta_{h2} - \delta_{h1})^2 \quad (6)$$

where 4 is an experimentally determined constant and the numbers 1 and 2 represent two different materials.

3.2.8 Calculation of die ratio

Die ratio, B_{swell}, of the extruded filaments was calculated using:

$$B_{swell} = d_e/d_d \quad (7)$$

where d_e is the extrudate diameter and d_d is the die diameter. In our case the d_d was 1.98 mm.

3.3 Chemical characterisation and morphology

3.3.1 Attenuated total reflectance-Fourier transform infrared spectroscopy (ATR-FTIR)

The ATR-FTIR spectra of the samples were obtained using a Perkin Elmer Frontier FT-IR Spectrometer (Waltham, MA, USA), which was equipped with a diamond GladiATR ATR attachment from Pike Technologies. For analysis, the samples were placed directly onto the ATR crystal without any additional preparation steps. The spectra were recorded in triplicates to ensure accuracy and reproducibility and were collected over a range of 4,000 to 400 cm^{-1} with a resolution of 4 cm^{-1} and an interval of 2 cm^{-1}, with 32 scans being collected for each sample. The ATR-FTIR measurement settings vary slightly across different studies; for more detailed information, please refer to the specific papers.

3.3.2 Scanning electron microscopy (SEM) and energy-dispersive X-ray spectroscopy (EDX)

The surface morphology of the pulp fibres in Paper I was examined using a field emission scanning electron microscope (SEM-FEI Quanta 200 FEG ESEM), Germany, equipped with an Energy-Dispersive X-Ray (EDX) spectrometer. To prepare the samples for imaging, they

were mounted on a strip of carbon tape and coated with a thin layer of conductive material. This preparation allowed for imaging under low-acceleration voltage (10 kV) and low-pressure conditions (0.2-1 bar) in the SEM chamber. The EDX analysis was performed to identify the elemental composition of the sample. The SEM imaging and EDX analysis helped to observe the surface features and changes in the chemical composition of the pulp fibres. For information regarding the acquisition of SEM images in Paper II and Paper III, please refer to the respective papers themselves.

3.3.3 Optical profilometry

TMP sheets of dimensions 3 cm x 3 cm were selected for this study. An optical profilometer (Sensofar S neox, Spain) was used to measure the surface roughness of the TMP sheets. The instrument uses a non-contact optical technique to measure surface with a high degree of accuracy and resolution. The samples were placed on the stage of the optical profiler. A 3D surface scan of 9 scans was performed for each sample.

3.4 Thermal properties

3.4.1 Thermogravimetric analysis (TGA)

The onset of thermal degradation was determined using a TGA/DSC 3+Star system (manufactured by Mettler Toledo, Switzerland). The specimens, weighing approximately 6 mg, were exposed to a heating ramp at a rate of 10°C per minute in a nitrogen atmosphere with a flow rate of 20 mL/min, ranging from 25 to 500°C.

3.4.2 Differential scanning calorimetry (DSC)

The thermal transitions and the crystallinity of the materials were assessed using a Mettler Toledo DSC2 calorimeter equipped with a HSS7 sensor and a TC-125MT intercooler. The endotherms were recorded while the temperature was increased from -50°C to 160°C at a scan rate of 10°C/min with a nitrogen flow of 50 mL/min. The degree of crystallinity (Xc) was calculated as Equation 8

$$X_c = \frac{\Delta H_c}{w_{EAA}\Delta H_o} \tag{8}$$

where ΔH_c is the specific heat of fusion of the composite, w_{EAA} the weight fraction of the matrix and ΔH_o the specific heat of fusion for 100 % crystalline PP; 209 J/g.[80]

3.5 Characterising mechanical properties and rheological properties of composite materials

3.5.1 Tensile testing

Tensile test bars, having a gauge length of 20 mm, were prepared from the compression-moulded specimens. The tensile properties, including Young's modulus, stress at break and elongation at break, were evaluated at room temperature with a strain rate of 6 mm/min using a Zwick/ Z2.5 tensile tester. The grip-to-grip separation was set at 40 mm and a load cell of 2 kN. In Paper I and Paper II two different instruments was used for practical reasons. For more information, please see each specific paper.

3.5.2 Dynamic mechanical analysis (DMA)

The dynamic mechanical properties of the samples were evaluated at room temperature (25°C) using a Rheometrics RSA II at a frequency of 1 Hz. The samples were subjected to a pre-straining under tension of approximately 0.15%, which was kept constant during the measurements. The sinusoidal deformation was applied with a strain amplitude that was incrementally increased from approximately 0.009% to 0.14%.

3.5.3 Notched Izod impact strength test

The impact strength of the notched Izod specimens was evaluated according to ISO 180 standards using a Tinius Olsen Model 92T plastics impact tester equipped with a 0.936 kg pendulum.

3.5.4 Rheology

Oscillatory shear rheology measurements were conducted using a DHR-3 (TA Instruments, USA) with a parallel plate geometry (diameter = 25 mm, gap = 4000 μm) at a temperature of 180°C. The temperature was controlled using an environmental test chamber (ETC) provided by TA Instruments. The measurements were taken at a strain of 0.25% over a frequency range of 0.1 to 100 Hz.

3.6 Friction measurements

A TA instrument rheometer manufactured in the USA and equipped with a 3 balls on plate (3BOP) configuration, was used to investigate the influence of AKD and MgSt on the frictional behaviour between metal and TMP sheets. The rheometer's geometry comprised three stainless steel hemispheres, each having a diameter of 6.3 mm. To conduct the experiments, paper sheets were securely affixed to the lower plate using a combination of double-sided tape and customised clamps (for more information see Paper III). This ensured stable immobilization of the sheets during the experiments. The investigations were carried out at different temperatures (30, 100 and 180 °C) using an environmental test chamber provided by TA instruments to maintain constant temperature conditions. Before each measurement, the zero gap was determined separately for each temperature setting. The COF was subsequently determined during sliding experiments at a constant sliding distance of 50 m, a velocity of 100 mm/s and an axial force of 1 N. The COF was calculated based on Equation 9, where F_f represents the frictional force and N denotes the normal force.

$$COF = \frac{F_f}{N} \tag{9}$$

3.7 Statistical analysis

Statistical analysis was conducted using the Origin data analysis software (OriginLab Corporation, Northampton, MA, USA), employing a one-way analysis of variance (ANOVA) test to assess differences among multiple groups. Significance level was set at $p < 0.05$.

4 Results and Discussion

4.1 Characterisation of TMP and modified TMP surfaces

4.1.1 Molecular surface fingerprint after modifications

The adsorption of MgSt and MoS_2 onto TMP fibres was investigated based on the EDX analysis of the samples. Figure 4 gives a graphical presentation of the elemental distribution of carbon (C), oxygen (O), magnesium (Mg), sulphur (S) and molybdenum (Mo) in each corresponding sample. In the case of TMP fibres with MgSt (Figure 4a), the presence of Mg was identified in regions exhibiting higher carbon intensity. This observation implies the coexistence of Mg and carbon-rich molecules like alkanes, providing evidence for the adsorption of MgSt onto the TMP samples.

Figure 4b depicts the elemental composition of 95 wt% TMP + 5 wt% MoS_2, revealing a matching distribution of Mo and S. This finding serves to confirm the presence of MoS_2 within the samples. Thus, the study demonstrates the adsorption of MgSt and MoS_2 onto TMP fibres through detailed elemental mapping.

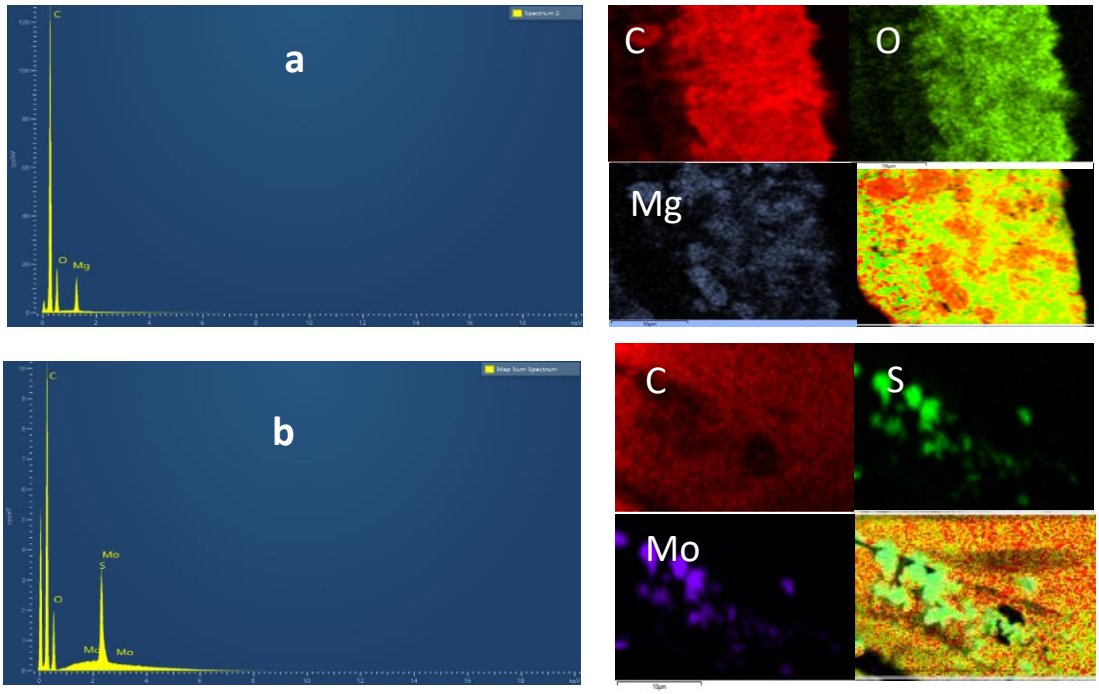

Figure 4. EDX analyses of 95 wt% TMP with (a) 5 wt% MgSt and (b) 5 wt.% MoS_2, elemental mapping of C, O, Mg, S and Mo and the combination of the components.

The investigation into IR spectra of TMP subjected to AKD modification unfolded through two approaches. Initially, various AKDs encompassing differing carbon chains were synthesised, namely AKD Hex, AKD Lau and AKD St (Figure 5a), with subsequent comparison of the resulting spectra (Paper II). I then conducted an investigation, wherein TMP fibres were subjected to variable quantities of commercial AKD (Paper III) applied as a spray (Figure 5b).

Figure 5a presents the IR spectra of unmodified TMP and TMP subjected to modifications using AKD Hex, AKD Lau and AKD St. Peaks at 2845 and 2916 cm^{-1} were observed, characteristic of carbon chains. This increase in intensity was particularly prominent for AKD Lau and AKD St modifications, whereas AKD Hex showed a modest enhancement. This variation suggests that the modification efficiency of TMP with AKD Hex is low compared to AKD Lau and AKD St. An important observation is the appearance of a new carbonyl peak at 1720 cm^{-1}, indicating the successful modification of TMP fibres through the incorporation of AKD Lau and AKD St.

Figure 5b illustrates the spectral profiles of TMP and TMP treated with varying quantities of commercial AKD. In this case, the carbonyl and carbon chain peaks were again observed.

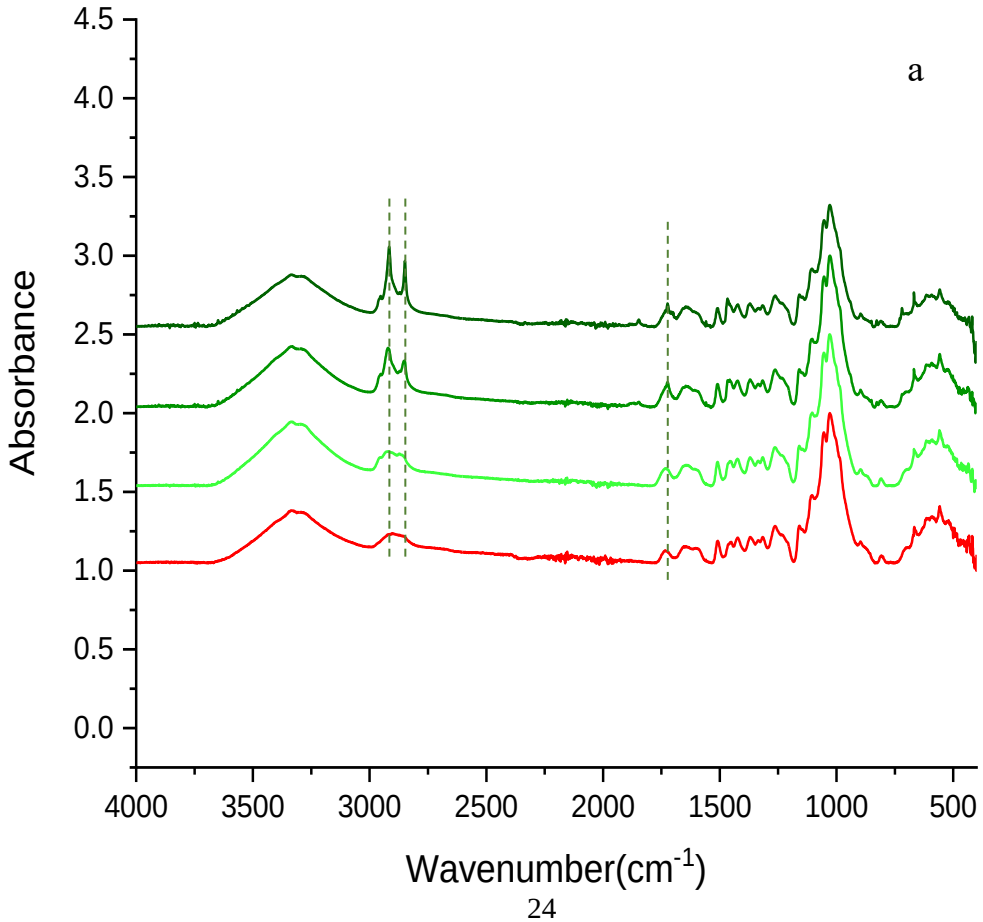

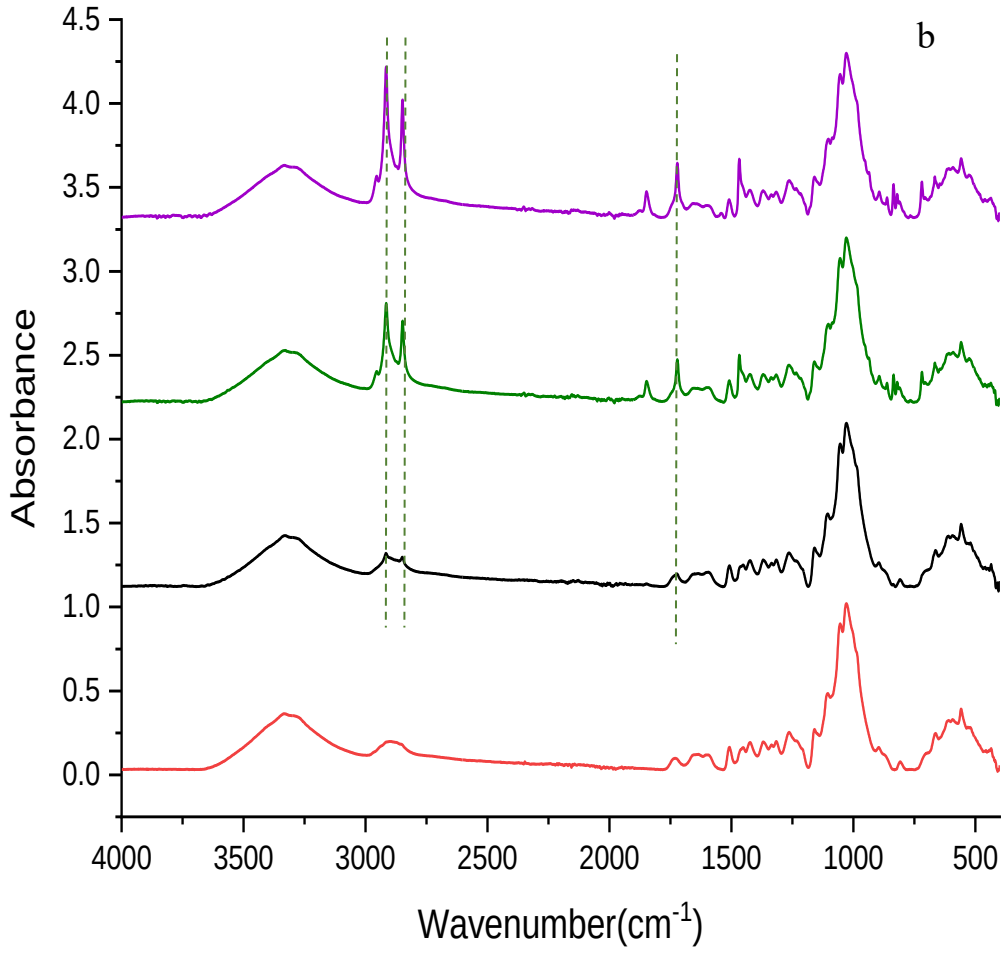

Figure 5. a) IR spectra of TMP (red), TMP AKD Hex, TMP AKD Lau and TMP AKD St respectively with different shades of green, with the light green being TMP AKD Hex and the darkest green TMP AKD St. b) IR spectra of TMP (red), TMP AKD0.5 (black), TMP AKD2 (green) and TMPAKD5 (purple). Dotted lines are added at the wavenumbers of 2916, 2845 and 1720 cm^{-1}.

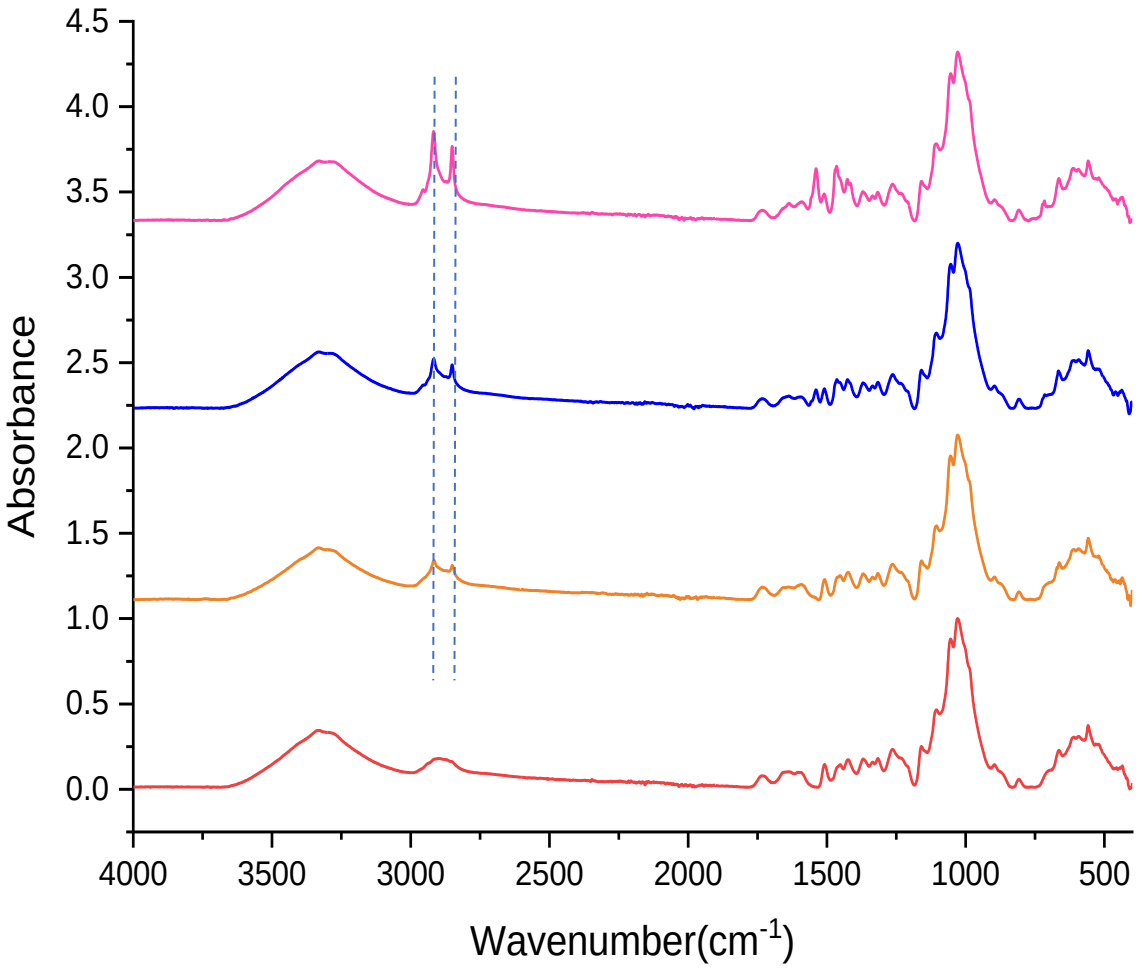

Figure 6) IR spectra of TMP (red), TMP MgSt0.5 (orange), TMP MgSt2 (blue) and TMP MgSt5 (pink), The spectra have been shifted by 1.2 units relative to each other to facilitate their separation and visualisation. Dotted lines are added at wavenumbers 2916 and 2845 cm^{-1}.

Figure 6 shows the IR spectra of TMP subject to sprayed MgSt. The amplification of intensity within the 2845 and 2916 cm^{-1} mirrors the earlier trends, underscoring a similar pattern of heightened carbon chain signals for TMP MgSt configurations.

4.1.2 Morphology and roughness of TMP fibre sheets

SEM micrographs were analysed to assess the impact of MgSt, MoS_2 and AKD on TMP fibres. Figure 7 shows SEM images of both a) TMP fibres and b) TMP fibres modified with MoS_2.

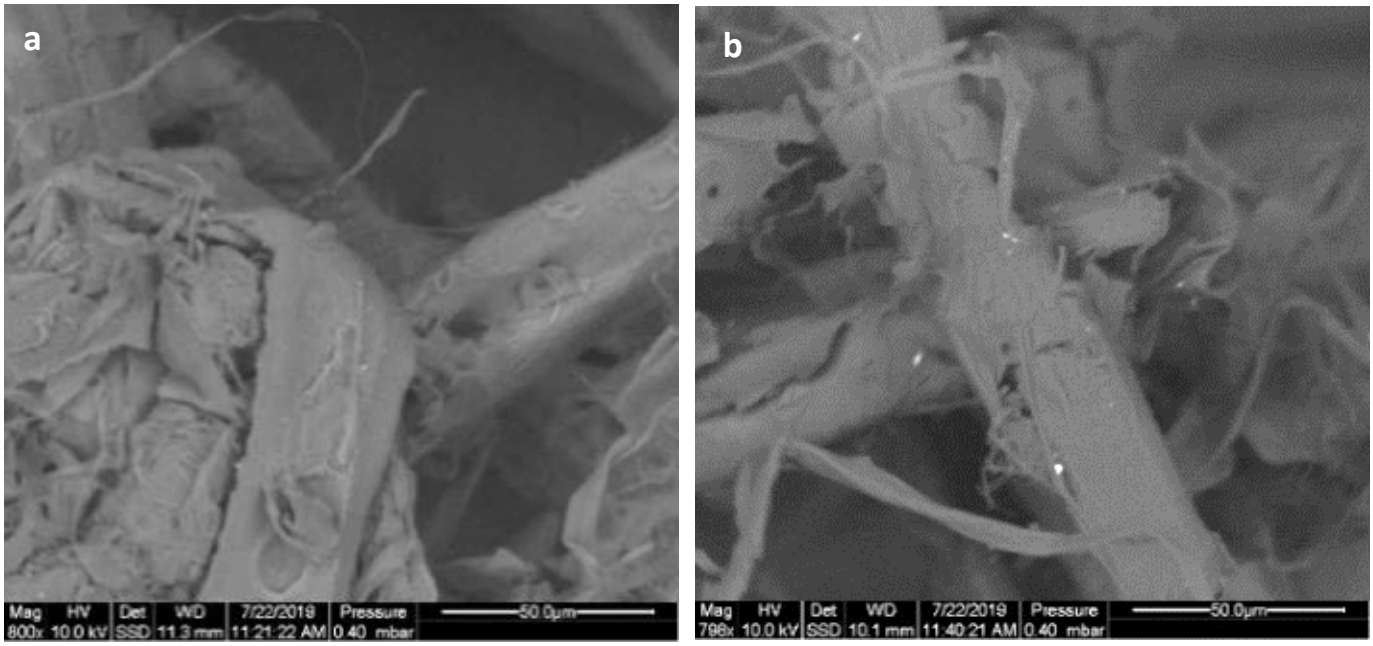

Figure 7. SEM images of (a) unmodified TMP fibres and (b) 95 % TMP+ 5 % MoS_2. Magnification: 800x.

In Figure 8, a series of SEM images unveils the impact of AKD and MgSt on the surface structure of TMP fibres. These images exhibit a distinctive pattern in the case of AKD, wherein the resultant particles manifest as numerous flat platelets that jointly produce spherical particles together. This phenomenon echoes observations from prior investigations[81,82] which elucidate similar platelet formations induced by the presence of AKD wax. Figures 8e and 8f show the deposition of MgSt. However, in this instance, the particles do not adopt spherical shapes.

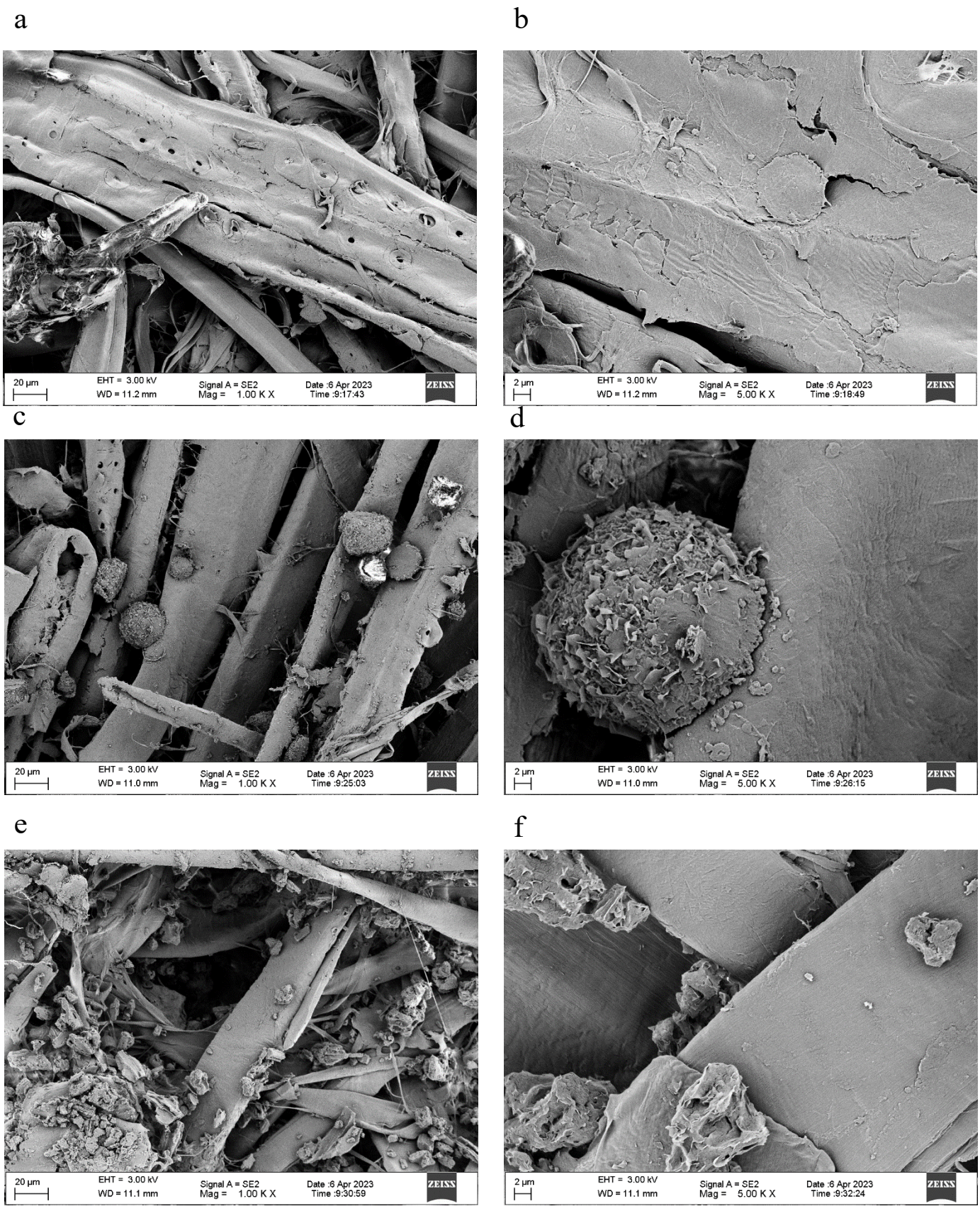

Figure 8. SEM images of TMP (a,b), TMP AKD5 (c,d) and TMP MgSt5 (e,f) at a magnification of 1000x (a,c,e) and 5000x (b,d,f).

The roughness of the TMP sheets sprayed with MgSt and AKD was assessed using optical profilometry, as shown in Figure 9. The results indicate there is no statistically significant variation in roughness across the samples. Therefore, the solvent used, nor the modifications made with AKD or MgSt had significant impact on the roughness of the surface of TMP fibres. The TMP sheets exhibit surface roughness ranging from 10% to 20% of their thickness, which, on average, measure 378 µm with a standard deviation of 46 µm.

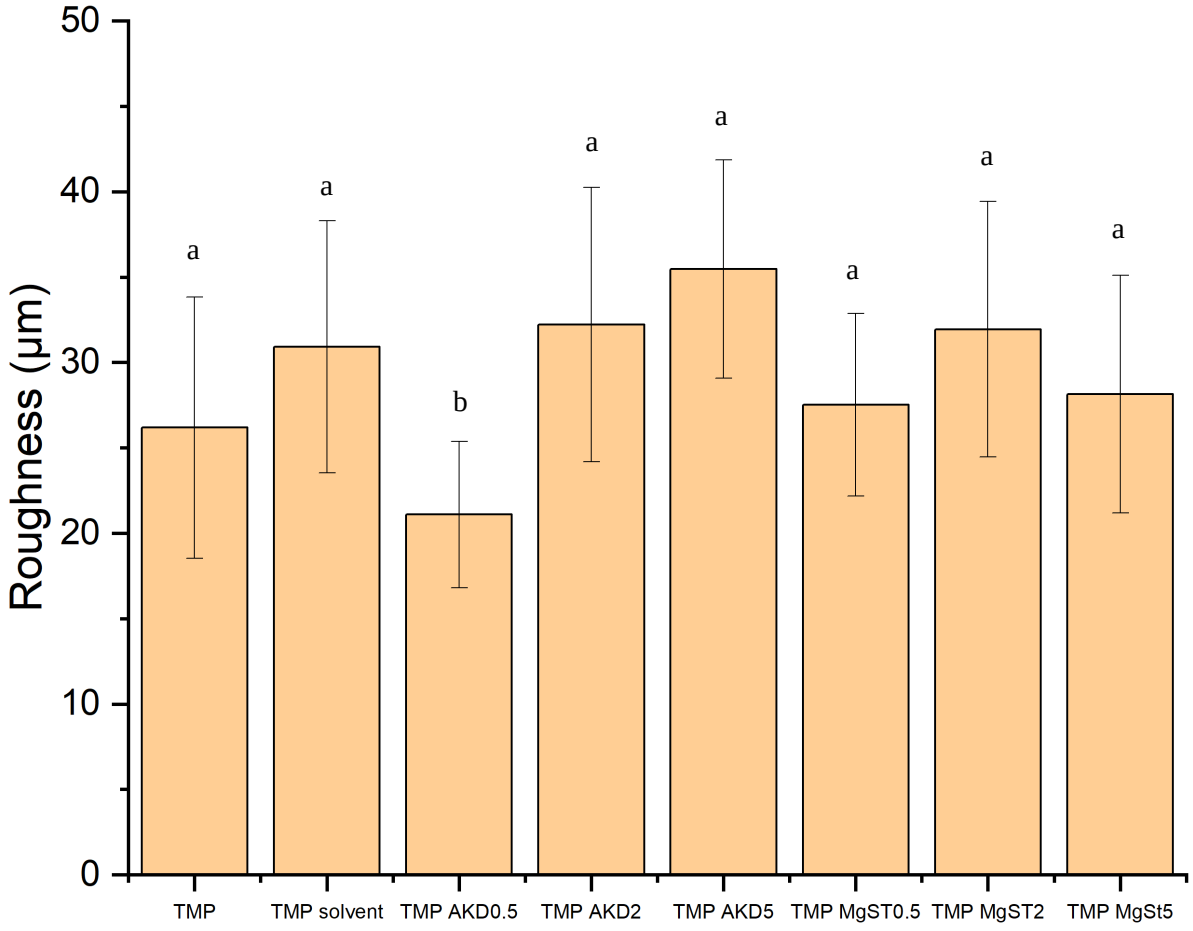

Figure 9. Roughness of TMP, TMP sprayed with solvent and TMP sprayed with solvent and additive (MgSt and AKD). Different letters above each column depict statistically significant difference ($p<0.05$).

4.1.3 The effect of AKD on surface interactions

The results presented in Table 4 reveal a change in how water interacts with TMP paper after the application of AKD. The contact angle was quantified as the angle formed at the initial point of contact between the drop and the surface of the sheet. When AKD with a longer carbon chain (AKD St) is used, the water's contact angle on the paper increases, reaching 126°. This is different from untreated TMP paper, where the contact angle is 83°. Assessments were conducted with other liquids like formamide, ethylene glycol and propylene glycol and it was found that their contact angles increased as AKD with longer carbon chains was used. These results suggest that AKD modification can increase the hydrophobicity of TMP paper sheets, as with previous observations using cellulose paper sheets.[83]

Table 4. The contact angle of distilled water (DW), a blend of DW and ethylene glycol, formamide, ethylene glycol and propylene glycol was measured on sheets prepared from TMP or AKD-modified TMP. The contact angles presented are the average of a minimum of eight measurements, with the standard deviation values provided within parentheses.

	Contact angle (º)				
Solvent / Sample	DW	DW/Ethylene glycol 50/50	Formamide	Ethylene glycol	Propylene glycol
TMP	83 (5)	71 (9)	54 (10)	56 (14)	53 (20)
TMP AKD Hex	105(13)	107 (10)	71 (11)	96 (13)	65 (13)
TMP AKD Lau	116 (11)	111 (8)	108 (10)	108 (11)	75 (11)
TMP AKD St	126 (9)	112 (12)	112 (4)	111 (10)	97 (11)

For the unmodified TMP fibres, the water droplet size and contact angle consistently decreased until the droplet was fully absorbed into the paper. However, with the modified TMP fibres, a different pattern emerged. The water droplet size and contact angle reached a stable point between 0.1 to 0.5 seconds after the droplet was placed (as shown in Figure 10). These findings reveal that the modified fibres behave differently when it comes to wetting which suggests the AKD modification enhances the fibres' resistance to water, and that the AKD with the longest carbon chain is most effective.

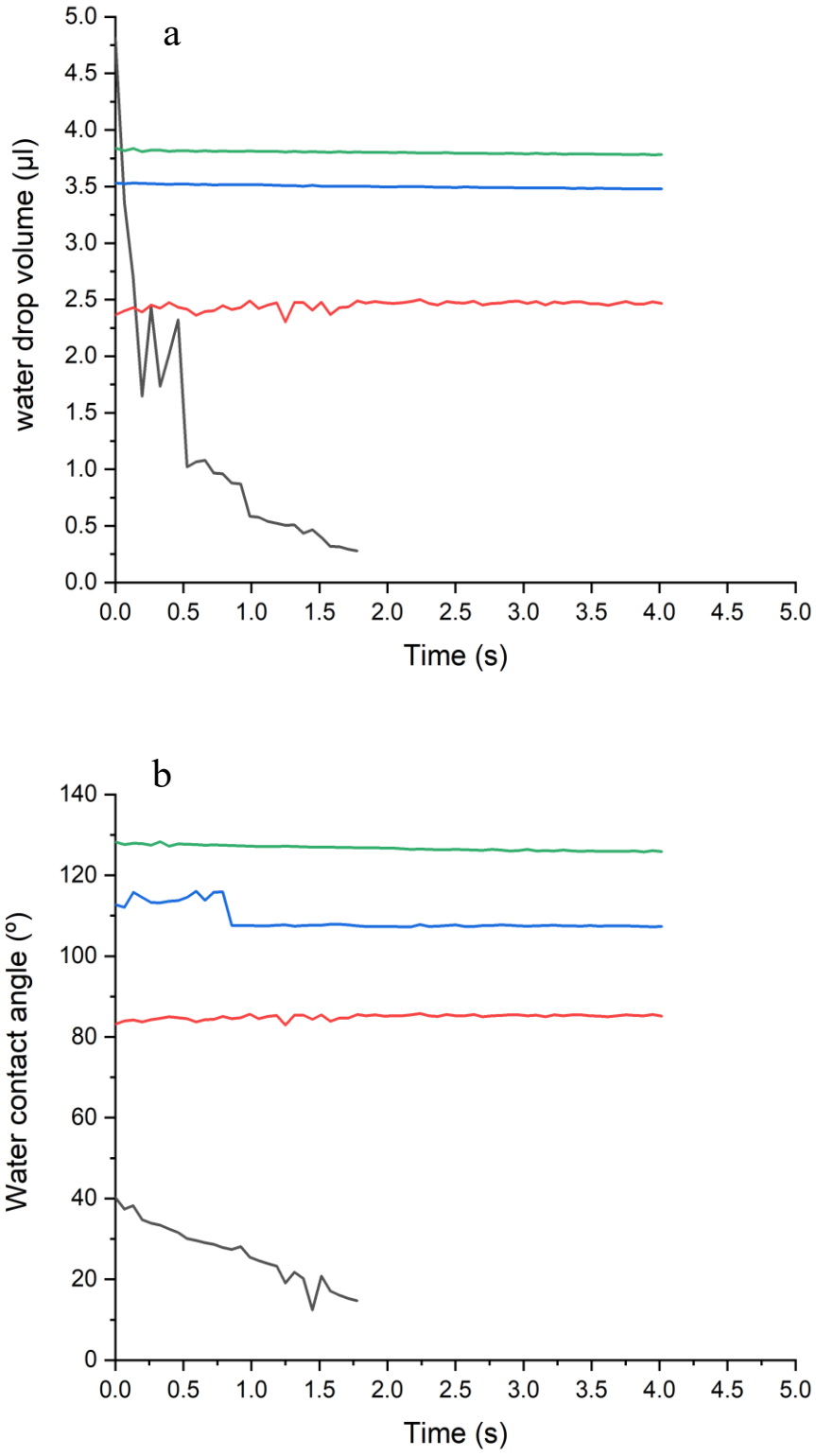

Figure 10. The changes in water drop volume (a) and water contact angle (b) TMP (black), TMP AKD Hex (red), TMP-AKD Lau (blue), TMP-AKD St (green)

Calculating of HSP serves as predicting solubility between different chemical compounds. Chemicals sharing akin to HSP values tend to exhibit comparable interactions. A study by Gårdebjer *et al.*[84] exemplified the applicability of HSP in forecasting the dispersibility of modified cellulose nanocrystals across diverse solvents and within a matrix polymer, specifically LDPE. This methodology was further extended to anticipate the compatibility between AKD and PP, and between cellulose-AKD and PP.

In our calculations involving cellulose-AKD in PP, an assumption was made that each cellulose unit would be linked to a single AKD molecule. The results shown in Table 5 outline the calculated HSP parameters. A noteworthy observation is that the HSP values gradually decrease as the carbon chain length of the AKDs increases. A distinct pattern in the total Hansen parameter squared (δ_{tot}^2), is also noticed. δ_{tot}^2, reflects the energy density per unit volume or the cohesive energy of the studied chemicals. This parameter consistently decreases as the AKD carbon chain length grows.

An essential factor here is the Ra value, a key measurement for comparing the partial Hansen solubility parameters between two different materials. A lower Ra indicates a higher theoretical solubility potential between the chemicals being studied. Table 5 shows a clear trend: the Ra value between AKD and PP decreases as the AKD side chain length increases. This connection suggests an increased theoretical ability of AKD to disperse within PP, thanks to the longer carbon chain. The opposite occurs when the Ra between water and AKD is examined. Here, the rising Ra values align with an increased hydrophobic nature, a characteristic that intensifies as the AKD carbon chain lengthens. While the HSP has been calculated based on cellulose rather than TMP, it is believed that most of the AKD interaction with TMP occurs between AKD and cellulose within TMP. Therefore, the results are expected to apply to TMP fibres as well.

Table 5. HSP parameters, the total HSP and Ra for AKD Hex, AKD Lau, AKD St, cellulose-AKD Hex, cellulose-AKD Lau and cellulose-AKD St in PP and water.

Sample	δ_D $[(J/cm^3)^{1/2}]$	δ_P $[(J/cm^3)^{1/2}]$	δ_H $[(J/cm^3)^{1/2}]$	δ_{tot} $[J/cm^3]^{1/2}$	Ra in PP	Ra in water
AKD Hex	17.5	2.8	6.3	18.8	7.0	38.5
AKD Lau	17.1	1.3	4.4	17.7	4.9	40.8
AKD St	17.0	0.9	3.5	17.4	4.2	41.7
Cellulose-AKD Hex	19.1	4.2	14.9	24.6	15.7	30.6
Cellulose-AKD Lau	18.1	2.3	11.2	21.4	11.4	34.4
Cellulose-AKD St	17.7	1.6	9.3	20.1	9.5	36.2
PP (Hansen)	18	3	3	18.5	41.7	41.7
Water (single molecule)[85]	15.5	16	42.3	47.8	39.2	0

4.2 Compression moulding and extrusion of TMP-additive-matrix

The TMP and TMP modified with AKD underwent a compounding process lasting 10 minutes. This compounding was carried out using a mini compounder operating at a pressure of 150 kN and a temperature of 190°C. The outcome, depicted in Figure 11, illustrates a reduction in filament roughness upon the introduction of AKD. This effect is particularly pronounced when using AKDs with longer carbon chains, such as AKD Lau and AKD St.

Earlier investigations have established a link between smoother filaments and the mitigation of shear pressure buildup within the extruder during the fabrication of polyethylene wood composites.[86]

Figure 11. A visual impression of filaments composed of a) PP-TMP b) PP-TMP AKD Hex c) PP-TMP AKD Lau and d) PP-TMP AKD St, as compounded for 10 minutes and extruded at 150 kN and 190 °C.

B_{swell} values are reduced following the modification of TMP with AKD, as illustrated in Table 6. This trend aligns with the observations of Ariffin et *al.*[87] who explored the interplay between shear stress and B_{swell}, noting an upward trend in B_{swell} with escalating shear stress.

Table 6. The diameter of extrudate filaments and die swell numbers are based on the average of 10 measurements.

Sample	Diameter (mm)	B_{swell}
PP-TMP	2.14 (0.07)	1.08 (0.04)
PP-TMP AKD Hex	2.02 (0.03)	1.02 (0.02)
PP-TMP AKD Lau	2.00 (0.03)	1.01 (0.02)
PP-TMP AKD St	1.99 (0.03)	1 (0.02)

Figure 12 presents a visual comparison of dog-bone samples produced from three materials: PP-TMP, modified PP-TMP composites and pure PP. Even though the TMP AKD Lau and AKD St samples contain a lower proportion of PP (but same proportion of TMP, that is 50 wt%), they exhibit a brighter colour than the unmodified TMP sample.

In wood-based composites, the common dark colour is often linked to localised thermal degradation during processing.[88–90] The brighter samples observed in the TMP/PP composites treated with AKD Lau and AKD St suggests a more favourable processing scenario, hinting at reduced thermal degradation. This lighter appearance shows the potential benefits of AKD modifications.

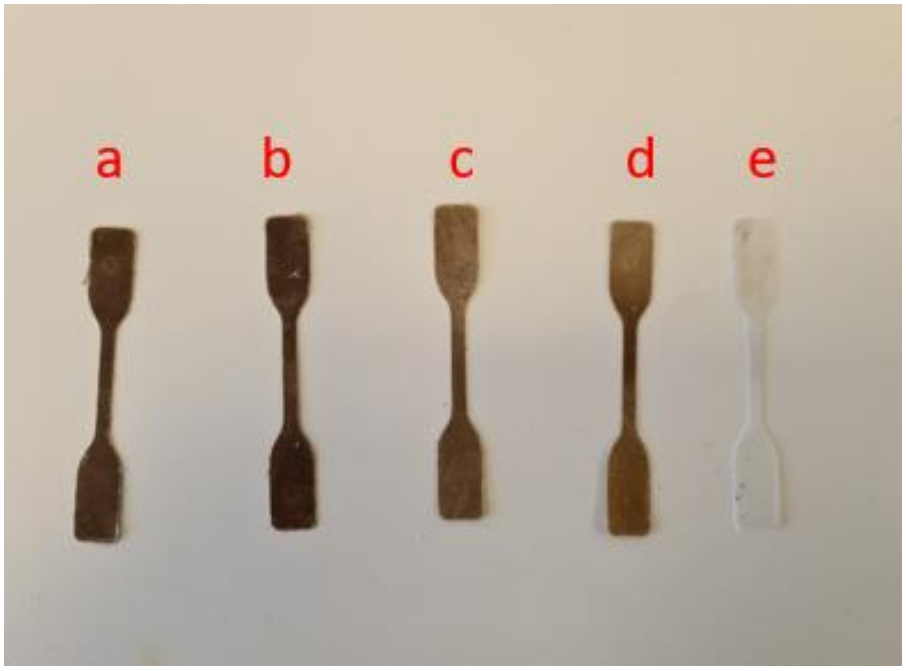

Figure 12. Hot-melt-compressed dog-bones of a) PP-TMP b) PP-TMP AKD Hex c) PP-TMP AKD Lau d) PP-TMP AKD St and e) PP filaments.

4.3 Thermal properties and crystallinity of unmodified and AKD modified TMP

The thermal stability of the TMP modified with AKD Hex, AKD Lau and AKD St was evaluated and results show a decrease in thermal stability as seen from the reduction in average onset temperature (T_{onset}) and final residual char (Table 7).

Table 7. The average T_{onset} and residual char content of the unmodified TMP and modified TMP fibres. Four repetitions were done for all samples. The SD values are in parentheses.

Sample	Residual Char (%)	T_{onset} (°C)
TMP	19 (0)	289 (0)
TMP AKD Hex	20 (2)	290 (2)
TMP AKD Lau	16 (4)	280 (6)
AKD TMP St	14 (0)	252 (0)

When the crystallinity of PP within the composite materials is examined, little change is observed and it remains in the range of 40-43 %. This indicates that TMP and AKD have a minor impact on the overall crystalline structure of PP.

However, AKD does affect the melting curve of PP (Figure 13). This suggests that AKD disrupts the crystalline arrangement of PP, causing it to melt at different temperatures. In essence, AKD introduces changes to PP's crystalline properties, which in turn distinctively influences its thermal behaviour.

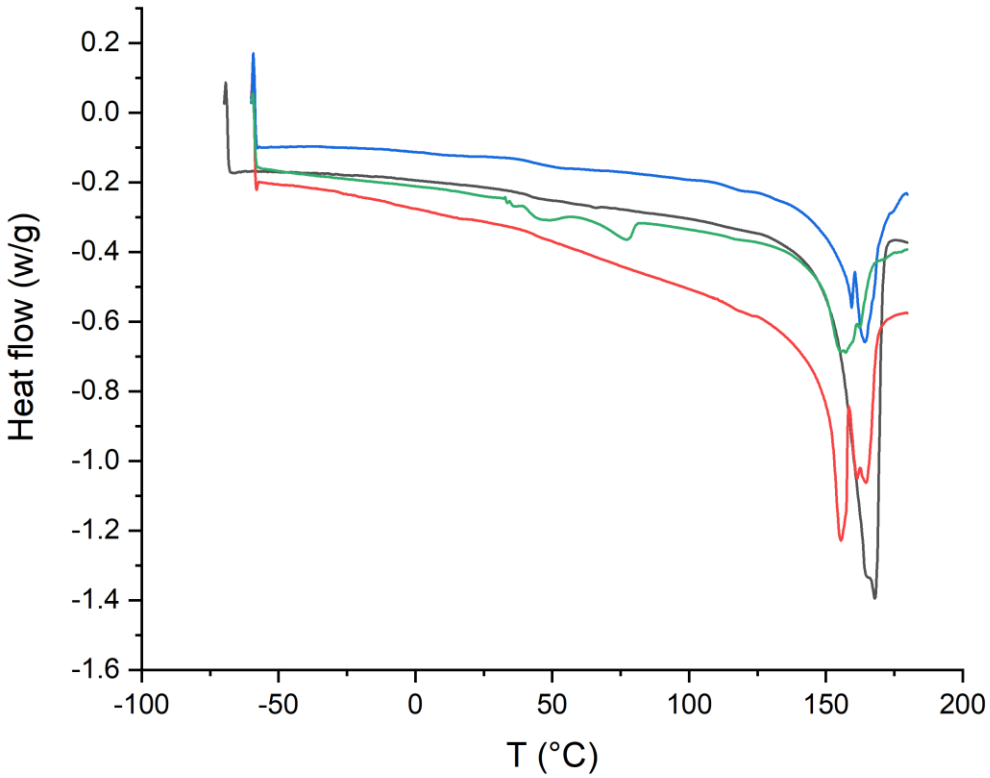

Figure 13. First melting curve of PP (black), PP-TMP AKD Hex (red), PP-TMP AKD Lau (blue) and PP-TMP AKD St (green) from DSC results.

4.4 Mechanical properties and rheology of the composites

4.4.1 Evaluating mechanical performance

Table 8 presents a comprehensive analysis of the impact of MgSt and MoS_2 on the mechanical properties of the composites. The highest Young's modulus was observed at the reinforcement of 70 wt% TMP. This improvement, an increase of 8.1 times relative to the matrix, shows the reinforcing efficacy of TMP. The introduction of additives at the reinforcement of 70 wt% brings about an even more substantial increase, elevating Young's modulus by a factor of 10.7 within the TMP-based specimens enriched with MoS_2.

The composites reinforced only with TMP, without any additives, demonstrate a rise in stress at break. It increases from 24 MPa (EAA) to 28 MPa for 30 wt% TMP composite and further to 38 MPa for 50 wt% TMP composite, as outlined in Table 8.

However, it is important to note that adding TMP without additives results in a drop in elongation at break. This situation improves when MgSt or MoS_2 were introduced, not only increasing elongation at break but also influencing stress at break and impact strength, particularly for the 30 wt% TMP composites.

At a higher TMP content (70 wt%), despite the increase in Young's modulus, there is a small change in strength and elongation. To explore additive effects further, the percentage of the additives were increased in the TMP30 samples. In summary, the findings highlight the positive role of MgSt and MoS_2 as additives in enhancing the mechanical properties of TMP-based composites. The most significant increases are seen at a 30 wt% TMP content with 1.5 wt% additive. Among these, the TMP30 composites enriched with MoS_2 exhibit the most notable increases in Young's modulus and strength. This could be attributed to interactions between lignin and MoS_2, promoting better distribution and bonding between TMP and the matrix. However, it is worth noting that when the additive dosage is raised to 5 wt%, samples containing MgSt show decreased Young's modulus and strength.[76]

Table 8. Mechanical properties of the TMP-based composites with EAA as the matrix. The reported values are the averages of five independent measurements, with the standard deviation in parentheses.

Sample	Young's modulus (GPa)	Stress at break (MPa)	Elongation at break (%)	Izod impact strength (kJ/m^2)
EAA	0.3 (0.06)	24 (1)	491 (20)	------
EAA-TMP30	1.4 (0.1)	28 (2)	4 (1)	6 (1)
EAA-TMP30-MgSt	1.5 (0.1)	35 (2)	5 (1)	7 (1)
EAA-TMP30-MoS_2	1.2 (0.1)	33 (1)	6 (1)	8 (1)
EAA-TMP30-MgSt/MoS_2	1.2 (0.1)	33 (3)	5 (3)	10 (1)
EAA-TMP30-5MgSt	1.4 (0.1)	32 (3)	4 (0.1)	7 (1)
EAA-TMP30-5MoS_2	1.6 (0.1)	39 (1)	5 (0.1)	11 (2)
EAA-TMP30-2.5(MgSt+MoS_2)	1.3 (0.1)	27 (3)	3 (0.4)	7 (2)
EAA-TMP50	2.2 (0.03)	38 (1)	3 (1)	
EAA-TMP50-MgSt	1.7 (0.08)	30 (5)	3 (1)	
EAA-TMP50-MoS_2	1.8 (0.3)	29 (3)	3 (1)	
EAA-TMP50-MgSt/MoS_2	1.6 (0.3)	27 (4)	3 (1)	
EAA-TMP70	2.4 (0.4)	33 (11)	3 (1)	
EAA-TMP70-MgSt	2.9 (0.4)	32 (6)	2 (1)	
EAA-TMP70-MoS_2	3.1 (0.1)	31 (6)	3 (1)	

When incorporating TMP into PP at a 50 wt% ratio, the resulting composite materials exhibit comparable strength at break and a reduction in elongation at break is observed (Figure 14). This decrease in elongation at break aligns with established findings when TMP fibres are introduced into composites.[76,91–94]

The modification of TMP with AKD Lau yields composites with stress and elongation at break akin to unmodified PP-TMP composites. The utilisation of AKD St as a modifier leads to a reduction in stress (Figure 14a). This decline in tensile strength at break may arise from factors such as reduced crystallinity, inadequate dispersion of fibres within the matrix, or compromised adhesion between the fibre and matrix. The examination of crystallinity in both pure PP and composite materials reveals a consistent degree of crystallinity across all compositions (as detailed in Figure 13). Thus, reduced crystallinity does not account for the observed weakening of the PP-TMP AKD St composite.

A study by Quillin *et al.*[18] investigated the modification of bleached kraft cellulose pulp using extended-chain AKDs. Their work showcased improved dispersion of cellulose within a surface-modified PP matrix featuring poly (vinyl alcohol). Despite this, a decline in composite strength was observed, attributed to a hypothetical reduction in hydrogen bonding between AKD-modified cellulose fibres and the surface-modified PP featuring poly (vinyl alcohol) matrix. It is worth noting that the incorporation of AKD (both AKD St and AKD Lau) into PP itself results in materials with decreased stress at break compared to pure PP (Figure 14b).

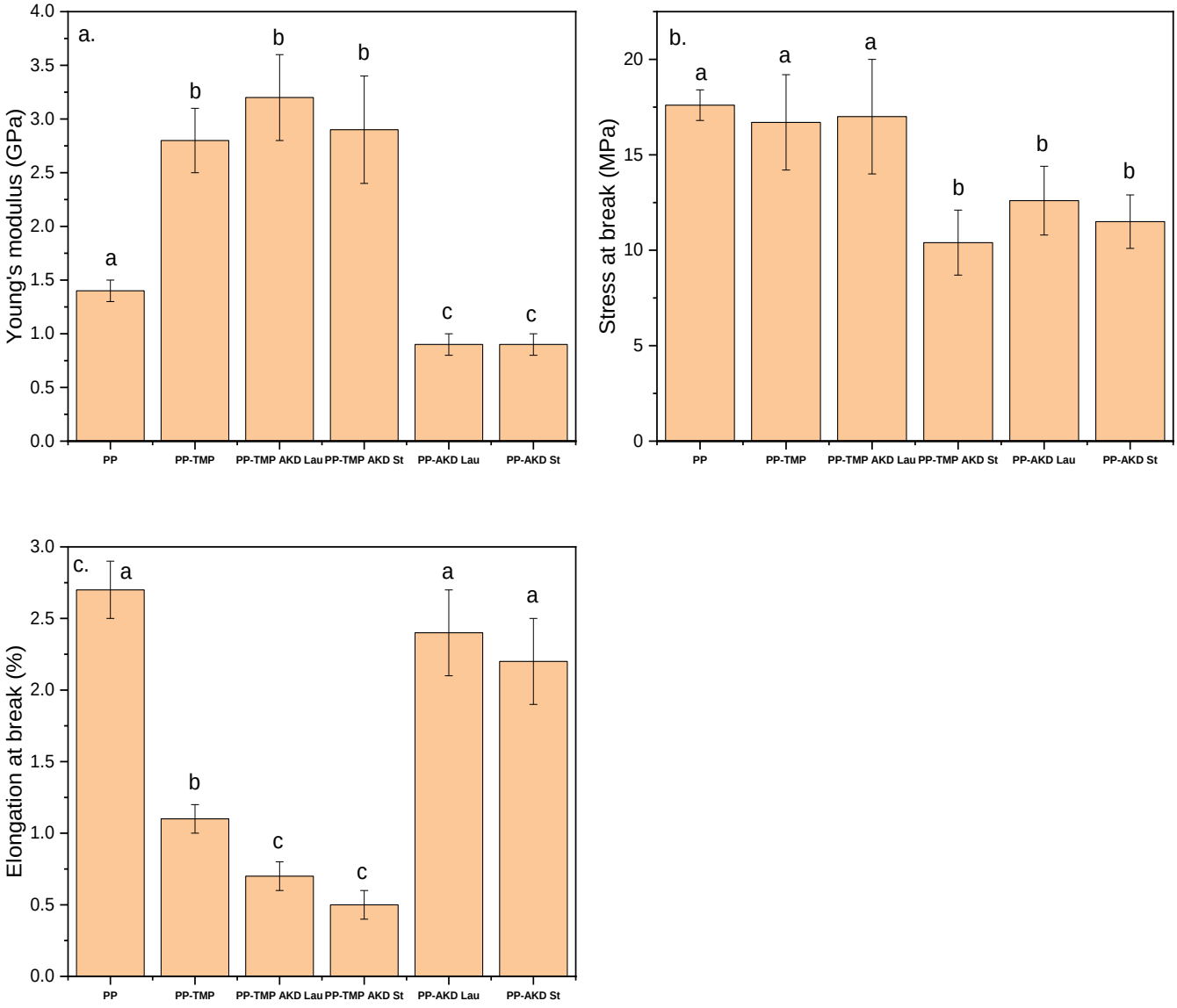

Figure 14. Mechanical properties of the composites: (a) Young's modulus, (b) strength at break and (c) elongation at break, with five repetitions done for each sample. The standard deviations are represented as black vertical lines for each bar and the SD is calculated based on five repetitions. Different letters above each column depict statistically significant differences ($p<0.05$).

4.4.2 The effect of additives on the viscoelasticity of the TMP composites

The damping factor, denoted as tan δ, serves as a valuable indicator of the interfacial characteristics within composite materials. A higher tan δ value implies a less favourable interface quality.[95,96] The investigation reveals that the tan δ of the 70 wt% TMP composites (Figure 15) surpasses that of the lower TMP load composites and exhibits an augmentation with increasing strain amplitude. This rise in the gradient of the loss factor curve (Figure 15) indicates the presence of a weakened interface region.

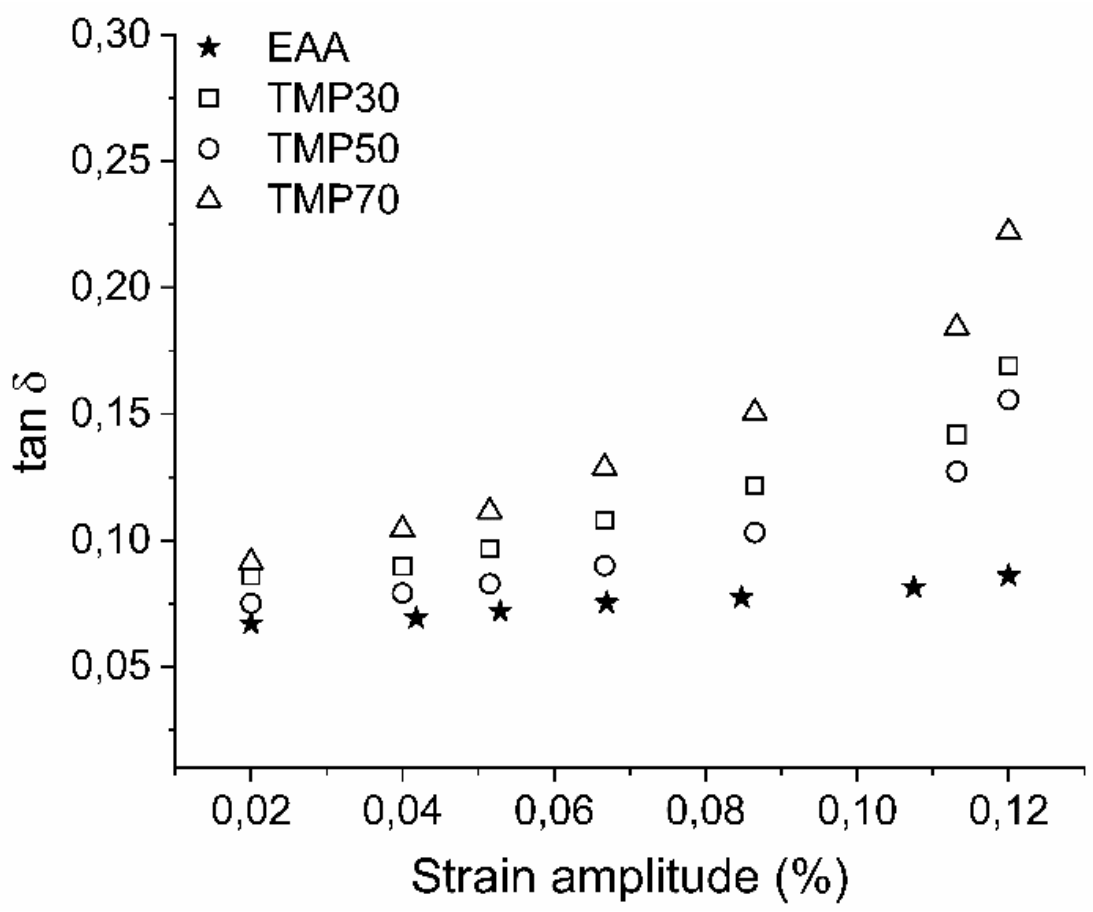

Figure 15. Damping factor as a function of the applied strain for composites with 30, 50 and 70 wt% TMP with EAA.

Figure 16a presents the properties of composites containing TMP and various additives. Except for the samples containing MgSt, the 30 wt% TMP composites with additives and their combinations exhibited a tan δ response to strain amplitude like that of the sample without additives. This suggests a relatively stable interphase region. However, the MgSt-containing

sample displayed an initial plateau up to a certain strain amplitude, followed by an increase in the tan δ slope. This indicates a more stable interphase region compared to the other composites at low strain amplitudes. In Figure 16b, representing composites with 70 wt% TMP, the slopes remained relatively consistent as the strain amplitude increased. This suggests a less effective interphase region and is anticipated, due to the smaller proportion of EAA in these higher loading composites.

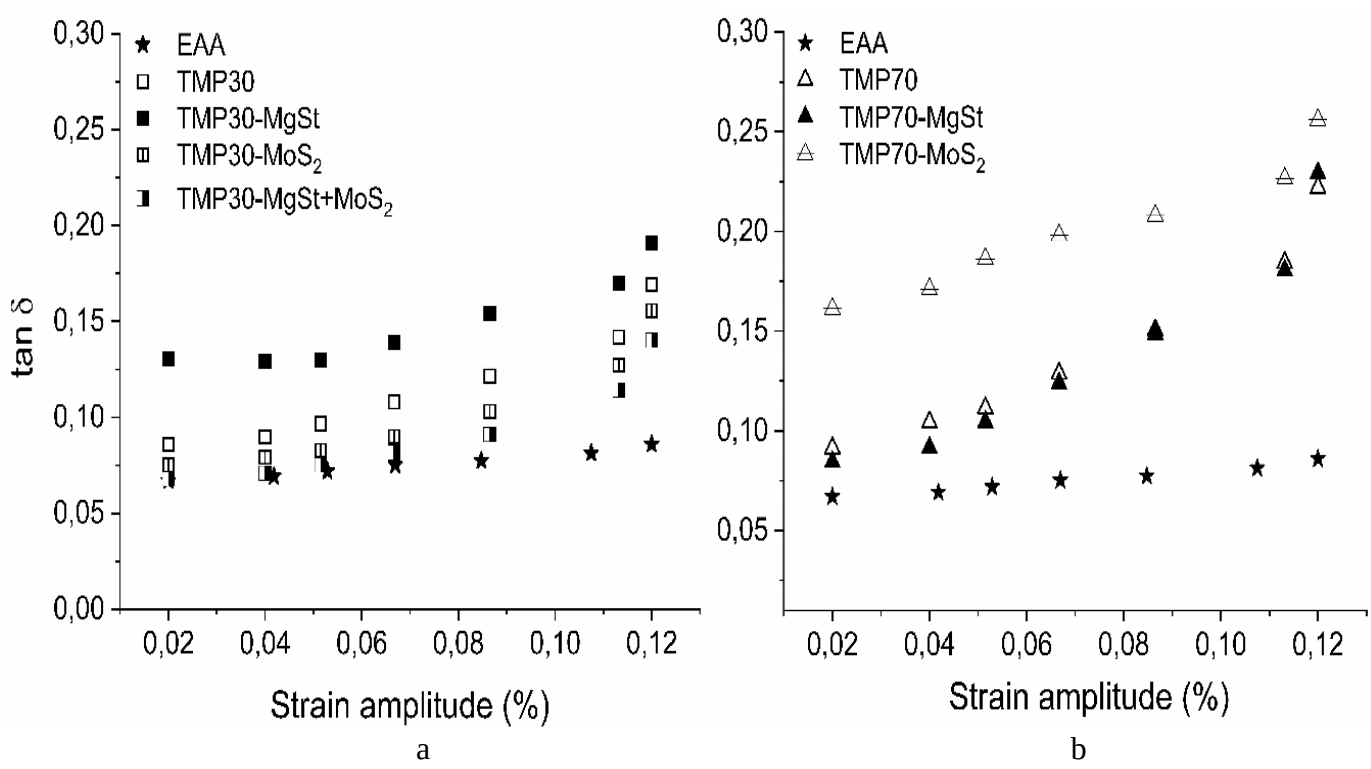

Figure 16. Mechanical loss factor as a function of applied strain amplitudes for (a) 30 wt% and (b) 70 wt% TMP samples with MgSt and/or MoS_2.

Figure 17 illustrates the impact of additive concentration on the mechanical loss factor of the TMP30 composite. As the MgSt concentration was increased from 1.5 wt% to 5 wt%, the tan δ slope and initial plateau observed at lower strain amplitudes with 1.5 wt% additive were no longer visible. These findings align with the mechanical properties presented in Table 8, where an overall decrease in mechanical performance was observed as the additive concentration in the composite increased. Conversely, when the MoS_2 concentration was raised, a plateau became apparent at higher strain amplitudes, which was not observed with 1.5 wt% MoS_2. This

relatively more stable interphase region corresponds with the observed increase in mechanical properties.

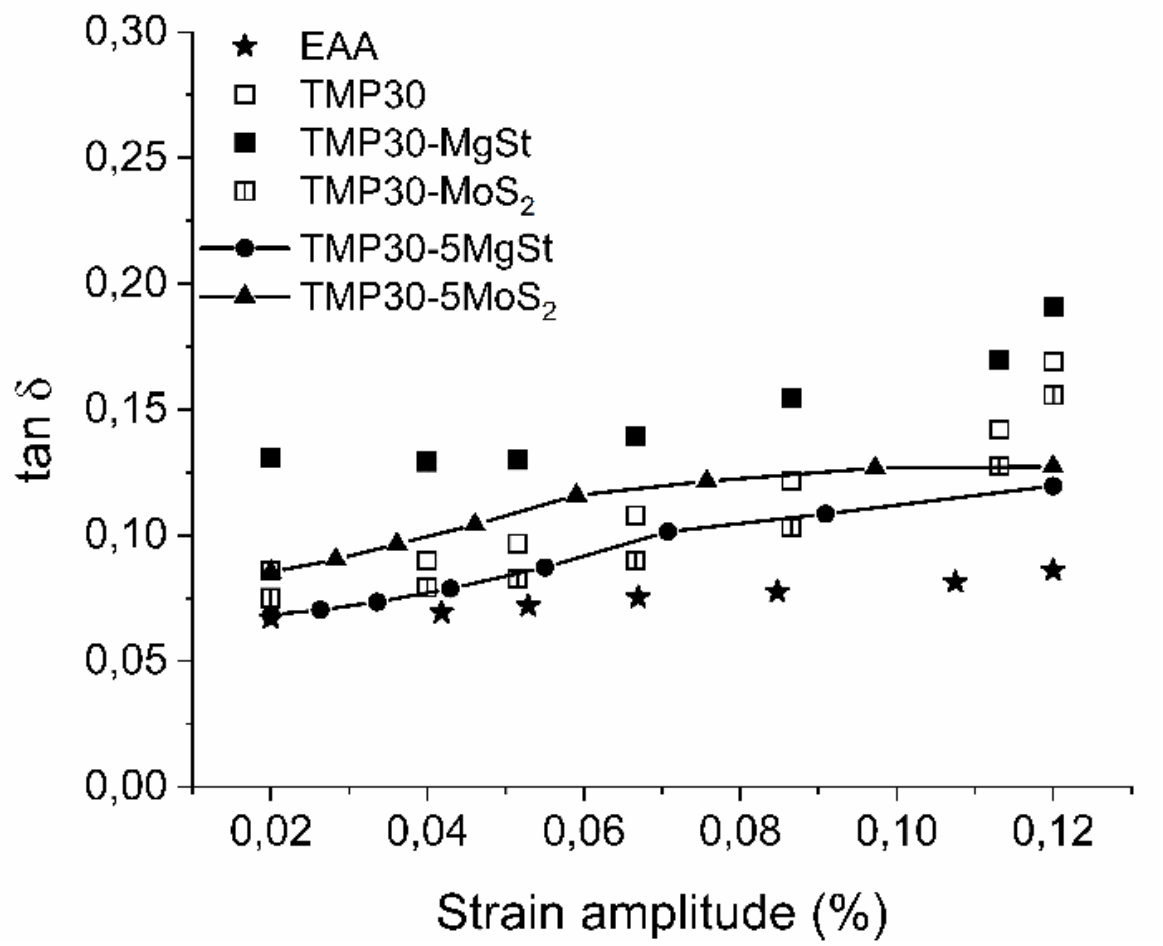

Figure 17. Mechanical loss factor as a function of applied strain amplitude for 30 wt% TMP samples with varying amounts of MgSt and MoS_2. The lines are as a visual guide only.

The decision to discontinue with AKD Hex was made based on the results from previous sections, which demonstrated the filament shapes and colours of dog-bones (Figures 11 and 12). Figure 18a illustrates the frequency-dependent behaviour of the storage (G') and loss (G") moduli for both pure PP and PP-TMP composites, measured at 180 °C. Pure PP behaves as a typical fluid, the moduli increase with frequency, and G" > G'. the moduli of the PP-TMP composites are consistently higher across the frequency sweep, compared to the pure PP and G' > G". This is in agreement with other studies[86,97–100] that have explored the impact of natural fibres on the rheology of fibre-matrix composites.

TMP and TMP AKD-modified composites demonstrate higher complex viscosities relative to pure PP. Modifying the samples with AKD St shows a slight reduction in complex viscosity with frequency. Initially, at low frequencies, the complex viscosity of the AKD St-containing sample aligns with that of the other specimens (PP-TMP and PP-TMP AKD Lau), registering at approximately 80 kPa·s at 1 rad/s. Nevertheless, at higher frequencies (300 rad/s), the complex viscosity of the AKD St-incorporated sample reduces to around 0.3 kPa·s, while its counterparts maintain complex viscosities of around 1 kPa·s (Figure 18b). It is noteworthy that no statistically significant variance is detected between the complex viscosity of PP-TMP AKD Lau and PP-TMP, as shown in Figure 18b.

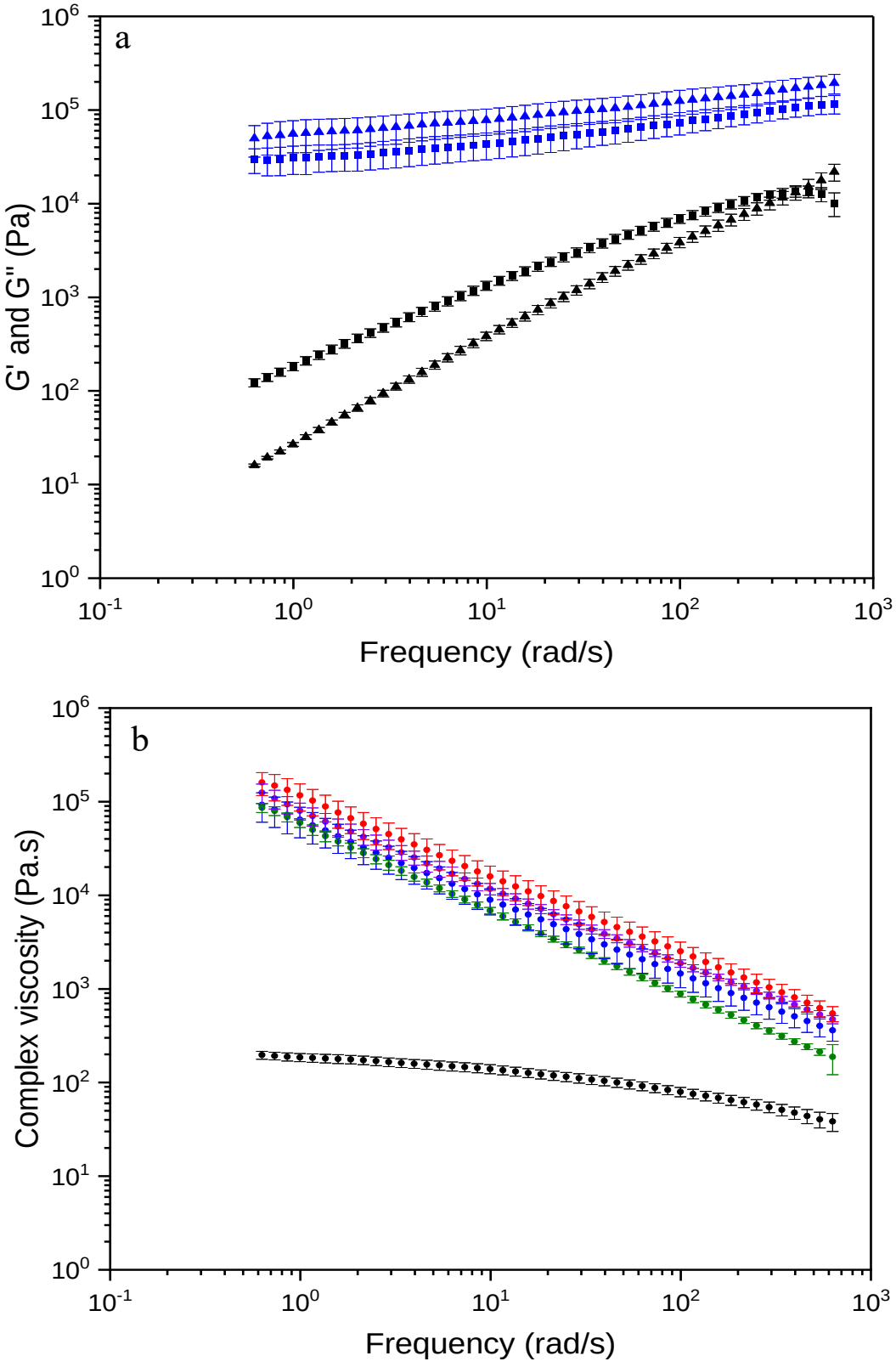

Figure 18. G' (triangles) and G" (squares), (a) and complex viscosity (circles), (b) as a function of frequency at T=180 °C and strain= 2.5 rad^{-1} for PP (black), PP-TMP (blue), PP-TMP AKD Lau (red) and PP-TMP AKD St (green)

The observed decline in complex viscosity could be attributed to the plasticising influence exerted by AKD St, which migrates into the PP matrix. This is corroborated by SEM images (see Paper II) displaying needle-shaped crystals indicative of unbound AKD St. In a bid to assess the plasticising effect of AKD on PP, melt viscosity was conducted on blends of PP AKD Lau and PP AKD St. As shown in Figure 19, both AKD Lau and St exhibit a plasticising effect on PP, leading to a reduction in complex viscosity by 30 Pa·s at a frequency of 300 rad/s.

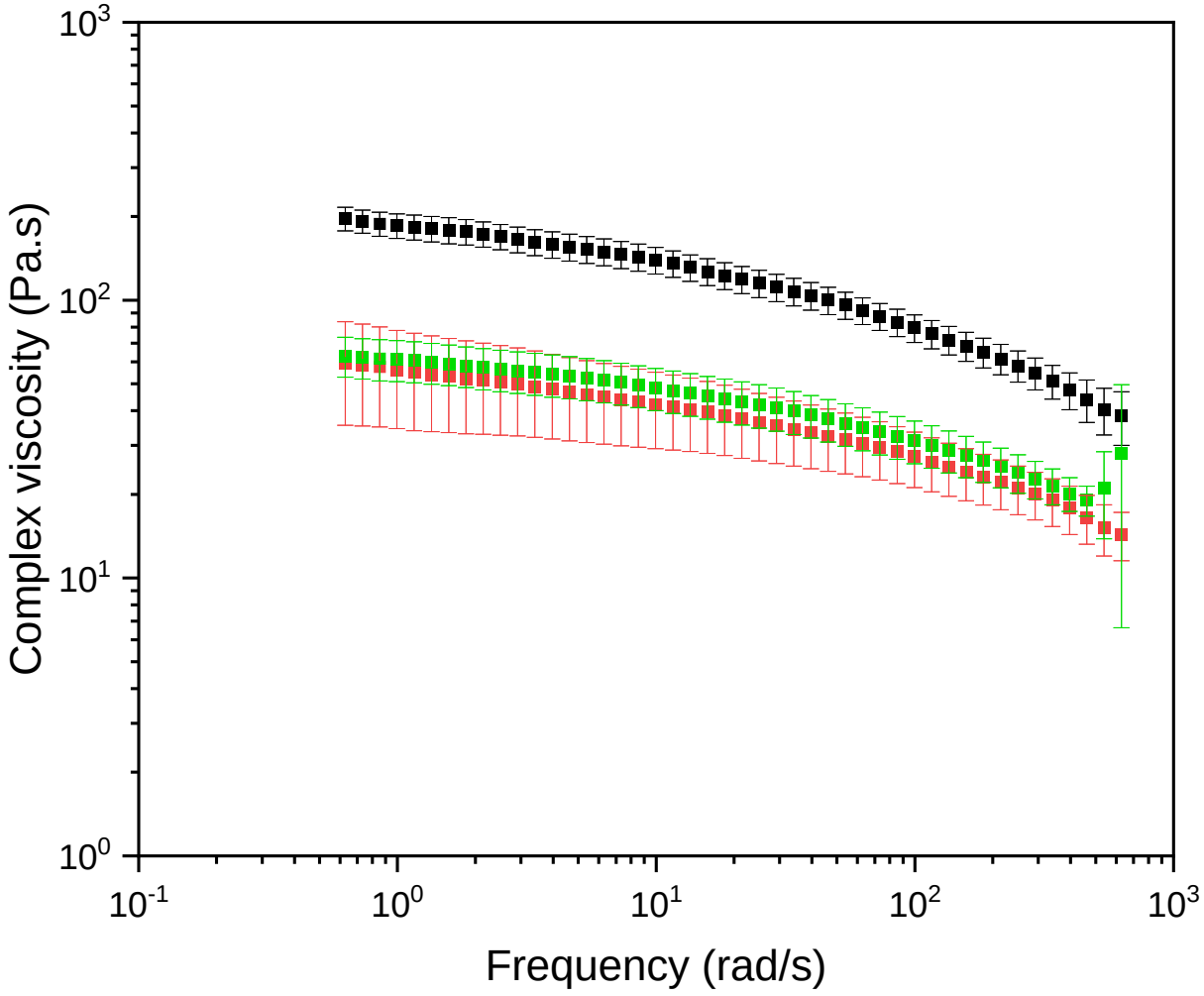

Figure 19. The complex viscosity as a function of frequency for PP (black), PP-AKD Lau (red) and PP-AKD St (green) at 180 °C.

4.5 Control of friction between TMP and metals using additives: Investigating the effect of AKD and MgSt on the friction between metal and TMP fibres

The average COF values for metal and TMP, metal and TMP with AKD, as well as metal and TMP with MgSt samples were determined at 30, 100 and 180 °C, with a sliding speed of 50 mm/s. Figure 20 illustrates a representative set of COF data over time for TMP-metal at 30 °C and these data points were used to calculate the average COF values.

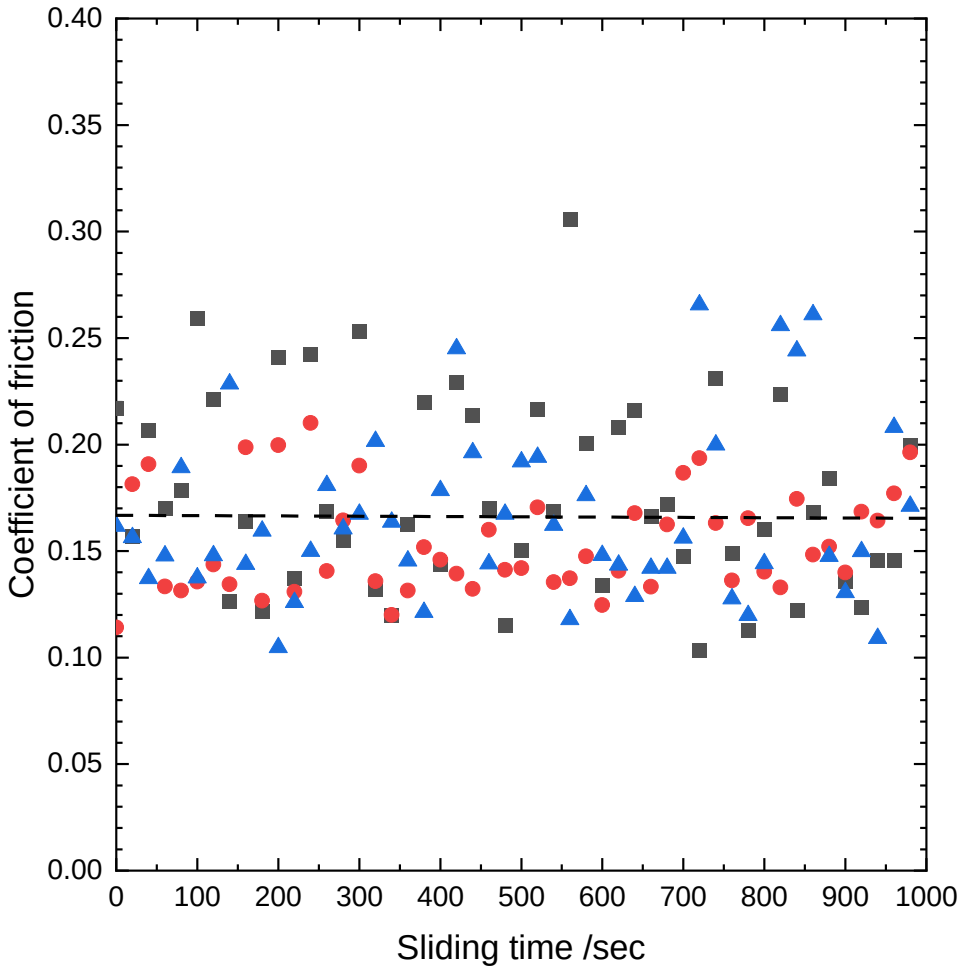

Figure 20. Coefficient of friction vs time for TMP-metal at T = 30 °C and at a speed of 50 mm/s where black squares, red circles and blue triangles depict three different measurements, resulting in the calculated average COF being 0.165 (dashed line) and standard deviation of 0.039.

COF between TMP and metal decreases as the temperature increases from 30 °C to 180 °C, as shown in Figure 21. Two potential explanations for this phenomenon exist: First, the lignin in the TMP sheet may soften as the temperature rises (starting at 100 °C), [101,102] second, exposure to higher temperatures may reduce the moisture content in the TMP sheet, which is known to decrease COF for metal-wood surfaces.[103] The thermogravimetric analysis of TMP (see Paper III for more details) demonstrates a 2.8% weight variation between temperatures of 30°C and 100°C for TMP, along with a smaller 0.5% weight difference between temperatures of 100°C and 180°C. This weight fluctuation is likely due to changes in moisture content. The friction test results show no statistically significant difference in the COF between TMP and metal at temperature range of 30°C to 100°C. However, at 180°C, the COF is lower compared to that at 100 and 30 °C. Considering the moisture content data, it appears unlikely that the reduction in COF at 180°C can be solely attributed to moisture content disparities.

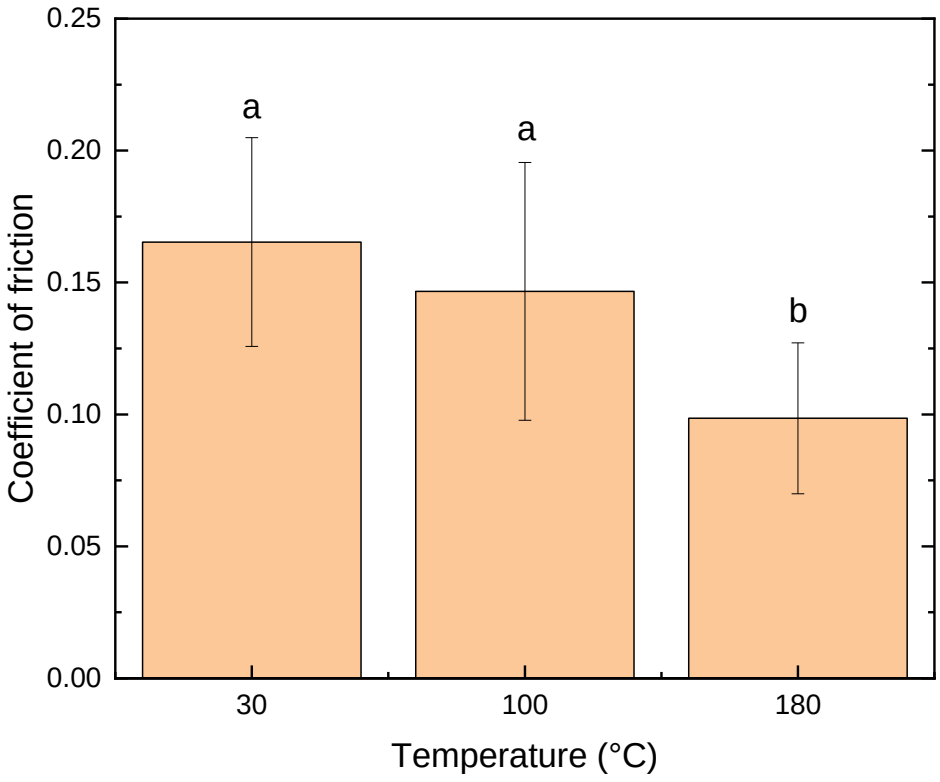

Figure 21. COF of TMP sheets and metal as a function of temperature. Different letters in each column show a statistically significant difference ($p<0.05$).

Figure 22 illustrates the impact of different concentrations of AKD and MgSt on the COF between metal and TMP sheets at various temperatures. At 30 °C, AKD0.5 has no significant effect on the COF between TMP and metal, while AKD2 and AKD5 reduce friction. Conversely, at the same temperature, all concentrations of MgSt increase friction between metal and TMP. At 100 °C, both AKD and MgSt, at any concentration, reduce the COF ($p<0.05$), with no notable difference between AKD and MgSt. At 180 °C, only AKD at 2 and 5 wt% reduces COF. At 0.5 wt%, the COF is statistically similar to that of TMP-metal alone at 180 °C. These results suggest that the additives effectively reduce COF only at higher temperatures. This reduction could be attributed to the additives dissolving during sheet preparation, migrating into the lignin and acting as plasticisers that soften the lignin further at elevated temperatures. However, it is noteworthy that the COF values at 100 and 180 °C are similar for 2 and 5 wt% AKD and MgSt. This suggests that the additives may not strongly influence the softening temperature.

At 30 °C, a decrease in COF is observed for AKD (except for AKD at 0.5 wt%) but not for MgSt. Even though AKD at 5 wt% has a rougher surface, it reduces friction compared to 0.5 wt%. Therefore, it can be inferred that neither the solvent nor any of the additives significantly affected the roughness of the TMP fibre surface.

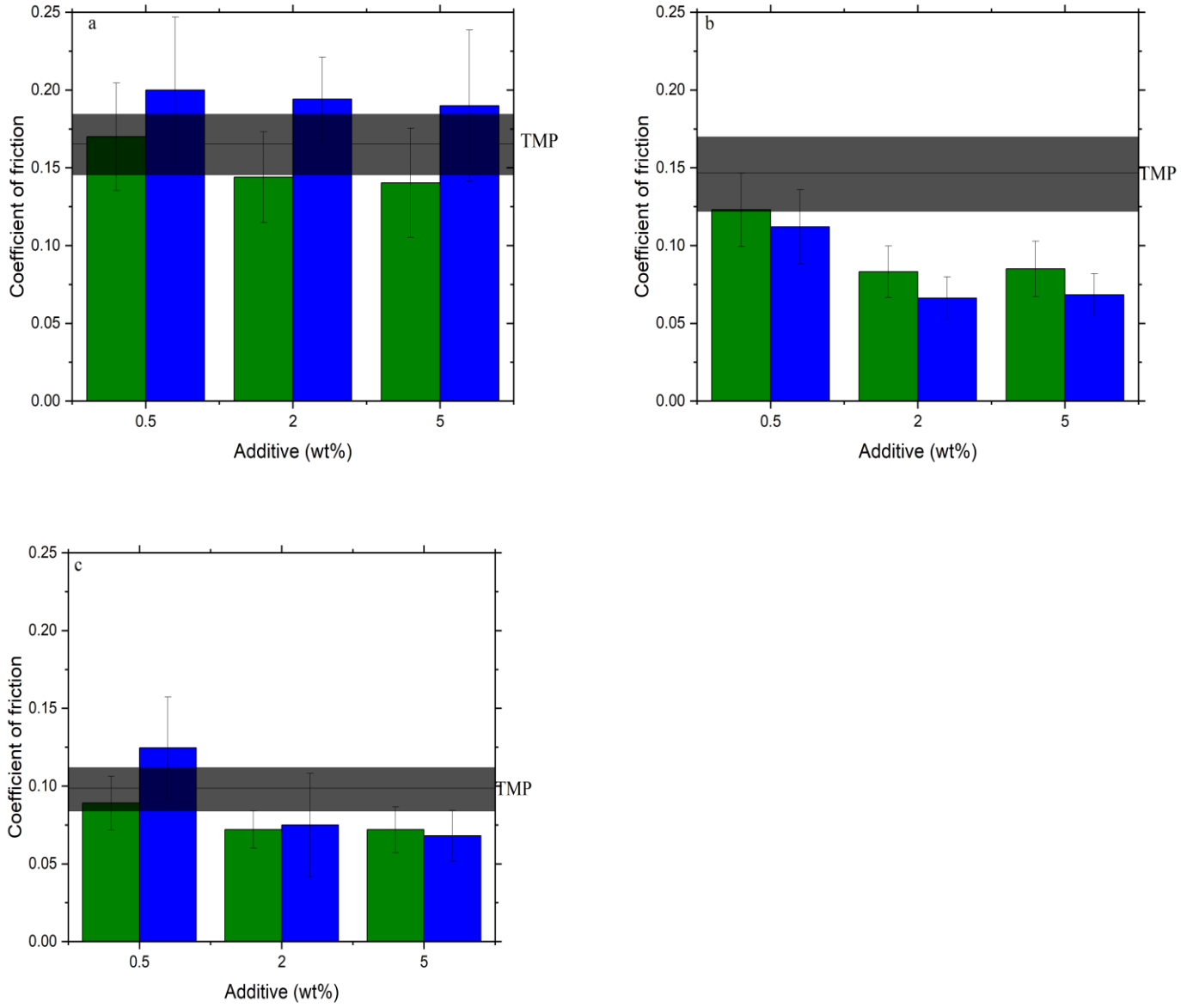

Figure 22. COF measurements between metal and TMP sheets with different added amounts of AKD or MgSt (wt%) for TMP AKD-metal (green) and TMP MgSt-metal (blue) at 30, 100 and 180 °C for (a), (b) and (c), respectively. For reference, the COF value of TMP-metal is shown by a straight line in each graph and a shadowed rectangle indicates the error bar.

5 Conclusions

In conclusion, the research conducted has investigated the potential improvements in TMP composites (processability and interface) with a high wt% of TMP, through various additives (MgSt, MoS_2 and AKD).

The findings indicate that MgSt and MoS_2 positively impacts the mechanical properties of the composites, particularly the tensile modulus. MoS_2 was more efficient with TMP-based samples compared to MgSt due to its interaction with lignin. Additionally, modifying the TMP surface with AKD increased hydrophobicity. Changes such as smoother die filaments, reduced discolouration of the composites and a subtle reduction in the composites' viscosity are indirect indications of the improving processability of the TMP composites when adding long-carbon-chain AKD.

The COF between metal and TMP at different temperatures was also investigated. High temperatures, 180°C, reduced the COF compared to lower temperatures (30°C). The addition of AKD reduced COF at all temperatures, while MgSt reduced COF at temperatures above 100°C.

The findings point to the possibility of processing high wt% TMP fibre composites by careful selection of additives. The combination of effective additives and a thorough understanding of their effect on the surface properties of TMP offers promising opportunities for advancing the industry and addressing practical challenges in the production of high wt% TMP-based composites.

6 Future work

Exploring alternative methods for interphase characterisation: although the influence of MoS_2 and MgSt on interfacial properties has been discussed based on DMA results in Paper I and theoretical HSP measurements were conducted in Paper II, it would be beneficial to investigate interphase properties using alternative methods such as the DMA fibre-pull out setup. This method allows for a deeper examination of the interactions between a single fibre and the matrix and the effect of the additives on this interaction.

Comprehensive analysis of TMP fibre interactions with the additives: TMP, composed of lignin, cellulose and hemicellulose, presents a complex composition. Further investigation into the interactions between TMP fibres and various additives can be beneficial. Dynamic FTIR spectroscopy may be used for this purpose, offering the capability to analyse molecular interactions within intricate polymeric systems. This analysis will help uncover how each additive interacts with the various components of TMP.

Investigation into the fibre-fibre friction: in Paper III, the impact of MgSt and AKD on the friction between metal fibres was examined. While understanding fibre-metal interactions during processing is crucial, another challenge lies in the entanglement of TMP fibres during the process. Therefore, it is imperative to investigate the effect of these additives on fibre-fibre friction. This research can potentially provide insights into strategies for reducing fibre entanglement by mitigating friction between the fibres.

A comprehensive analysis of the impact of reduced friction on surface defects: while Paper II demonstrates that AKD with a high carbon chain leads to a decrease in surface defects, and in Paper III I have hypothesized that the reduced friction between TMP fiber and metal by additives in processing temperature leads to decrease in surface defects, further investigation is needed. To address this, we can employ a method involving the establishment of controlled extrusion processing parameters, where the sole independent variable is the amount of previously validated additives known for their capacity to decrease friction between fibers and metal. Following this, we can carefully examine the filaments and compare surface defects.

7 Acknowledgments

With profound gratitude, I extend my heartfelt appreciation to those whose unwavering support and contributions have been the cornerstone of this doctoral thesis. This remarkable journey would not have been attainable without the collective encouragement and guidance of numerous individuals and institutions.

Foremost, my deepest thanks are extended to my dedicated academic supervisor, Anna Ström, whose steadfast support, invaluable mentorship and expert guidance have been the compass guiding my research odyssey. Anna's unwavering commitment to excellence and her generous sharing of knowledge have profoundly shaped my academic and research trajectory.

I extend my sincere appreciation to my co-supervisors, Anette Larsson and Gunnar Westman, whose expertise and assistance have enriched this journey. Likewise, I would like to express gratitude to my examiner, Lars Öhrström, for his valuable insights.

Acknowledgment is due to Itai Panas, the current director of studies and Lars Evenäs, the former director of studies, as well as Nina Kann, Assistant Head of Department at Chemistry and Chemical Engineering, who all provided essential support and guidance.

My heartfelt thanks are extended to Anders Mårtensson for his contributions in providing SEM images, as well as to Anders Brolin and Tobias Moberg from StoraEnso for their insightful discussions and guidance.

I owe a debt of gratitude to my cherished mentor, Sheila, for her invaluable assistance.

I wish to acknowledge the camaraderie and moments shared with my colleagues in applied chemistry, especially my dear friends Åke, Roujin, Giovanni, Sozan, Frida, Smaragda and my office mate, Julia. I am also deeply grateful for the unwavering support of my dear friends outside work, who have stood by me in both joyful and challenging times during these years of friendship.

I am immensely thankful for the financial support provided by VINNOVA, Sweden's innovation agency and StoraEnso, which has been instrumental in enabling this research.

My appreciation also extends to the dedicated staff and resources at the Department of Chemistry and Chemical Engineering, Chalmers University of Technology, who have facilitated the research process, offered technical assistance and fostered an environment conducive to academic growth.

To my dear parents, who I may not have had the opportunity to see often, but who always hold a special place in my heart.

I would like to express my heartfelt gratitude to Sweden and particularly to Gothenburg, which has been my home for the past five years. My journey here has had its share of ups and downs, but the beauty of this city and the warmth and kindness of its people have consistently provided me with the strength to rise again. I am truly amazed by the generosity and kindness of the Swedes.

Last but not least, I want to thank myself for believing in me, for doing all this hard work, for never quitting despite all the discouragements and dark moments that I experienced.

With profound gratitude and appreciation,

Skål!

Ehsan Hosseini

8 Bibliography

1. Brooks, A. L., Wang, S. & Jambeck, J. R. The Chinese import ban and its impact on global plastic waste trade. *Sci Adv* **4**, (2018).
2. Circular Economy: new rules on single-use plastics. *European Commission accessed at:* https://ec.europa.eu/commission/presscorner/detail/de/STATEMENT_19_1873 (2019).
3. The forest and sustainable forestry accessed at: *Swedish Wood accessed at:* https://www.swedishwood.com/wood-facts/about-wood/wood-and-sustainability/the-forest-and-sustainable-forestry/ (2019).
4. Li, Y. Wood-Polymer Composites. in *Advances in Composite Materials - Analysis of Natural and Man-Made Materials* 229–284 (IntechOpen, 2011).
5. Schirp, A. & Stender, J. Properties of extruded wood-plastic composites based on refiner wood fibres (TMP fibres) and hemp fibres. *Eur. J. Wood Prod.* **68**, 219–231 (2010).
6. Mertens, O., Gurr, J. & Krause, A. The utilization of thermomechanical pulp fibers in WPC: A review. *Journal of Applied Polymer Science* **134**, 45161 (2017).
7. Nygård, P., Tanem, B. S., Karlsen, T., Brachet, P. & Leinsvang, B. Extrusion-based wood fibre–PP composites: Wood powder and pelletized wood fibres – a comparative study. *Composites Science and Technology* **68**, 3418–3424 (2008).
8. Lu, J. Z., Wu, Q. & Negulescu, I. I. Wood-fiber/high-density-polyethylene composites: Compounding process. *Journal of Applied Polymer Science* **93**, 2570–2578 (2004).
9. Schirp, A., Mannheim, M. & Plinke, B. Influence of refiner fibre quality and fibre modification treatments on properties of injection-moulded beech wood–plastic composites. *Composites Part A: Applied Science and Manufacturing* **61**, 245–257 (2014).
10. Song, Y., Wang, Y., Li, H., Zong, Q. & Xu, A. Role of Wood Fibers in Tuning Dynamic Rheology, Non-Isothermal Crystallization, and Microcellular Structure of Polypropylene Foams. *Materials* **12**, 106 (2019).

11. Yuan, C., Michael, P., Kinkai, M., Shangbing, M. & Yunri, F. Method for incorporating wet natural fibers and starch into thermoplastics, patent. (2017).
12. Liu, W. *et al.* Lignin-assisted exfoliation of molybdenum disulfide in aqueous media and its application in lithium ion batteries. *Nanoscale* **7**, 9919–9926 (1394).
13. Donnet, C. & Erdemir, A. Historical developments and new trends in tribological and solid lubricant coatings. *Surface and Coatings Technology* **180–181**, 76–84 (2004).
14. Leinonen, U. I., Jalonen, H. U., Vihervaara, P. A. & Laine, E. S. Physical and lubrication properties of magnesium stearate. *J Pharm Sci* **81**, 1194–1198 (1992).
15. Wada, Y. & Matsubara, T. Pseudopolymorphism and lubricating properties of magnesium stearate. *Powder Technology* **78**, 109–114 (1994).
16. Varnell, D. F. Process for surface sizing paper and paper prepared thereby, patent. (2000).
17. Lindström, T. & Larsson, P. T. Alkyl ketene dimer (AKD) sizing : A review. *Nordic Pulp & Paper Research Journal* **23**, 202–209 (2008).
18. Quillin, D. T., Caulfield, D. F. & Koutsky, J. A. Cellulose/Polypropylene Composites: The Use of AKD and ASA Sizes as Compatibilizers. *International Journal of Polymeric Materials and Polymeric Biomaterials* **17**, 215–227 (1992).
19. Wang, Y. *et al.* Wear behavior and microstructure evolution in pure nickel extrusion manufacturing. *Transactions of Nonferrous Metals Society of China* **33**, 1472–1491 (2023).
20. Malkin, A. Y. & Patlazhan, S. A. Wall slip for complex liquids – Phenomenon and its causes. *Advances in Colloid and Interface Science* **257**, 42–57 (2018).
21. Marton, J. Practical aspects of alkaline sizing. On kinetics of alkyl ketene dimer reactions : hydrolysis of alkyl ketene dimer. *TAPPI JOURNAL* 139–143 (1990).
22. Seppänen, R. On the Internal Sizing Mechanisms of Paper with AKD and ASA Related to Surface Chemistry, Wettability and Friction, PhD thesis. (KTH, 2007).

23. Karademir, A., Hoyland, D., Wiseman, N. & Xiao, H. A Study of the Effects of Alkyl Ketene Dimer and Ketone on Paper Sizing and Friction Properties. *Appita : Technology, Innovation, Manufacturing, Environment* **57**, 116–120 (2004).
24. Biermann, C. J. 3 - Pulping Fundamentals. in *Handbook of Pulping and Papermaking (Second Edition)* (ed. Biermann, C. J.) 55–100 (Academic Press, 1996).
25. Park, J. *et al*. Use of mechanical refining to improve the production of low-cost sugars from lignocellulosic biomass. *Bioresource Technology* **199**, 59–67 (2016).
26. Hasani, M. Chemical modification of cellulose-new possibilities of some classical routes, PhD thesis. (Chalmers University of Technology, 2010).
27. Heinemann, S., Kleen, M., Wang, S. & Peltonen, J. Mechanical Pulping: Characterization of fiber wall surface structure of chemically modified TMP fibers from Norway spruce. *Nordic Pulp & Paper Research Journal* **26**, 21–30 (2011).
28. Kangas, H. & Kleen, M. Surface chemical and morphological properties of mechanical pulp fines. *Nordic Pulp & Paper Research Journal* **19**, 191–199 (2004).
29. Ciolacu, D. E. & Popa, V. I. CELLULOSE ALLOMORPHS – OVERVIEW AND PERSPECTIVES. in *Cellulose: Structure and Properties, Derivatives and Industrial Uses* 1–38 (Nova Science Publishers, Inc., 2010).
30. Gierlinger, N., Schwanninger, M., Reinecke, A. & Burgert, I. Molecular Changes during Tensile Deformation of Single Wood Fibers Followed by Raman Microscopy. *Biomacromolecules* **7**, 2077–2081 (2006).
31. Sjöström, E. *Wood chemistry: Fundamentals and applications*. (Academic Press, 1993).
32. Bajpai, P. Chapter 2 - Wood and Fiber Fundamentals. in *Biermann's Handbook of Pulp and Paper (Third Edition)* (ed. Bajpai, P.) 19–74 (Elsevier, 2018).

33. Biron, M. 1 - Outline of the Actual Situation of Plastics Compared to Conventional Materials. in *Thermoplastics and Thermoplastic Composites (Second Edition)* (ed. Biron, M.) 1–29 (William Andrew Publishing, 2013).
34. Dodiuk, H. & Goodman, S. H. 1 - Introduction. in *Handbook of Thermoset Plastics (Third Edition)* (eds. Dodiuk, H. & Goodman, S. H.) 1–12 (William Andrew Publishing, 2014).
35. Bledzki, A. K. & Gassan, J. Composites reinforced with cellulose based fibres. *Progress in Polymer Science* **24**, 221–274 (1999).
36. Liu, K., Zhang, C. & Madbouly, S. A. 10 - Fiber Reinforced Plant Oil-Based Composites. in *Bio-Based Plant Oil Polymers and Composites* (eds. Madbouly, S. A., Zhang, C. & Kessler, M. R.) 167–189 (William Andrew Publishing, 2016).
37. Duc, F., Bourban, P. E., Plummer, C. J. G. & Månson, J.-A. E. Damping of thermoset and thermoplastic flax fibre composites. *Composites Part A: Applied Science and Manufacturing* **64**, 115–123 (2014).
38. Ariño, R. & Boldizar, A. Processing and mechanical properties of thermoplastic composites based on cellulose fibers and ethylene—acrylic acid copolymer. *Polymer Engineering & Science* **52**, 1951–1957 (2012).
39. Bora, R. R., Wang, R. & You, F. Waste Polypropylene Plastic Recycling toward Climate Change Mitigation and Circular Economy: Energy, Environmental, and Technoeconomic Perspectives. *ACS Sustainable Chem. Eng.* **8**, 16350–16363 (2020).
40. Ragaert, K., Delva, L. & Van Geem, K. Mechanical and chemical recycling of solid plastic waste. *Waste Management* **69**, 24–58 (2017).
41. Geyer, R., Jambeck, J. R. & Law, K. L. Production, use, and fate of all plastics ever made. *Science Advances* **3**, e1700782 (2017).

42. Wu, J., Yu, D., Chan, C.-M., Kim, J. & Mai, Y.-W. Effect of fiber pretreatment condition on the interfacial strength and mechanical properties of wood fiber/PP composites. *Journal of Applied Polymer Science* **76**, 1000–1010 (2000).
43. Joseph, P. M. Effect of processing variables on the mechanical properties of sisal-fiber-reinforced polypropylene composites. *Composites science and technology* **59**, 1625–1640 (1999).
44. Oksman, K. & Lindberg, H. Interaction Between Wood and Synthetic Polymers. *Wood–Polymer Composites* **49**, 249–254 (1995).
45. Maldas, D. & Kokta, B. V. Influence of maleic anhydride as a coupling agent on the performance of wood fiber-polystyrene composites. *Polymer Engineering & Science* **31**, 1351–1357 (1991).
46. Bruce, R. W. *Handbook of Lubrication and Tribology, Volume II : Theory and Design, Second Edition*. (CRC Press, 2012).
47. Lee, S., Shupe, T. F. & Hse, C. Y. Thermosets as compatibilizers at the isotactic polypropylene film and thermomechanical pulp fiber interphase. *Composite Interfaces* **15**, 221–230 (2008).
48. Uzunovic, A. & Vranic, E. Effect of magnesium stearate concentration on dissolution properties of ranitidine hydrochloride coated tablets. *Bosnian J. Basic Med. Sci.* **7**, 279–283 (2007).
49. Odeniyi, M. A., Alfa, J. & Jaiyeoba, K. T. Effect of Lubricants on Flow Properties and Tablet Strength of Silicified Microcrystalline Cellulose. **33**, 71–75 (2008).
50. Dankovich, T. A. & Hsieh, Y.-L. Surface modification of cellulose with plant triglycerides for hydrophobicity. *Cellulose* **14**, 469–480 (2007).

51. Rozman, H. D., Khalil, H. P. S. A., Kumar, R. N., Abusamah, A. & Kon, B. K. Improvements of Fibreboard Properties through Fibre Activation with Silane. *International Journal of Polymeric Materials and Polymeric Biomaterials* **32**, 247–257 (1996).
52. Kazayawoko, M., Balatinecz, J. J. & Matuana, L. M. Surface modification and adhesion mechanisms in woodfiber-polypropylene composites. *Journal of Materials Science* **34**, 6189–6199 (1999).
53. Kazayawoko, M., Balatinecz, J. J. & Woodhams, R. T. Diffuse reflectance Fourier transform infrared spectra of wood fibers treated with maleated polypropylenes. *Journal of Applied Polymer Science* **66**, 1163–1173 (1997).
54. Schirp, A. & Schirp, C. Online Pre-Treatment of Thermomechanical Pulp with Emulsified Maleated Polypropylene for Processing of Extruded Thermoplastic Composites. *Fibers* **9**, 17 (2021).
55. Lee, S., Shupe, T. F., Groom, L. H. & Hse, C. Y. Thermomechanical pulp fiber surface modification for enhancing the interfacial adhesion with polypropylene. *Wood and Fiber Science, Vol. 39(3): 424-433* (2007).
56. Xie, H. *et al.* Highly compatible wood thermoplastic composites from lignocellulosic material modified in ionic liquids: Preparation and thermal properties. *Journal of Applied Polymer Science* **111**, 2468–2476 (2009).
57. George, M., Mussone, P. G. & Bressler, D. C. Surface and Bulk Transformation of Thermomechanical Pulp Using Fatty Acyl Chlorides: Influence of Reaction Parameters on Surface, Morphological, and Thermal Properties. *Journal of Wood Chemistry and Technology* **36**, 114–128 (2016).
58. Lindstrom, T. & O'Brian, H. On the mechanism of sizing with alkylketene dimers: Part 2. The kinetics of reaction between alkylketene dimers and cellulose. *Nordic Pulp & Paper Research Journal* **1**, 34–42 (1986).

59. Lenard, J. G. 9 - Tribology. in *Primer on Flat Rolling (Second Edition)* (ed. Lenard, J. G.) 193–266 (Elsevier, 2014).
60. Chaudhary, V., Bajpai, P. K. & Maheshwari, S. An Investigation on Wear and Dynamic Mechanical behavior of Jute/Hemp/Flax Reinforced Composites and Its Hybrids for Tribological Applications. *Fibers Polym* **19**, 403–415 (2018).
61. Bajpai, P. K., Singh, I. & Madaan, J. Frictional and adhesive wear performance of natural fibre reinforced polypropylene composites. *Proceedings of the Institution of Mechanical Engineers, Part J: Journal of Engineering Tribology* **227**, 385–392 (2013).
62. Devadas, A., Nirmal, U. & Hossen, J. Investigation into mechanical & tribological performance of kenaf fibre particle reinforced composite. *Cogent Engineering* **5**, 1479210 (2018).
63. Inoue, M., Gumagul, N. & Aroca, P. Static Mction properties of linerboard. *Tappi Journal* (1990).
64. Yousif, B. F. & Chin, C. W. Epoxy composite based on kenaf fibers for tribological applications under wet contact conditions. *Surf. Rev. Lett.* **19**, 1250050 (2012).
65. Chin, C. W. & Yousif, F. Influence of particle size, applied load, and fibre orientation on 3B-A wear and frictional behaviour of epoxy composite based on kenaf fibres. *Proceedings of the Institution of Mechanical Engineers, Part J: Journal of Engineering Tribology* **224**, 481–489 (2010).
66. Narish, S., Yousif, B. F. & Rilling, D. Adhesive Wear of Thermoplastic Composite Based on Kenaf Fibres. *Proceedings of the Institution of Mechanical Engineers, Part J: Journal of Engineering Tribology* **225**, 101–109 (2011).
67. Alshammari, F. Z. *et al.* The Influence of Fibre Orientation on Tribological Performance of Jute Fibre Reinforced Epoxy Composites Considering Different Mat Orientations. *Tribol. Ind.* **40**, 335–348 (2018).

68. Yallew, T. B., Kumar, P. & Singh, I. Sliding Wear Properties of Jute Fabric Reinforced Polypropylene Composites. *Procedia Engineering* **97**, 402–411 (2014).
69. Dwivedi, U. K. & Chand, N. Influence of Fibre Orientation on Friction and Sliding Wear Behaviour of Jute Fibre Reinforced Polyester Composite. *Appl Compos Mater* **16**, 93–100 (2009).
70. Behera, S., Gautam, R. K., Mohan, S. & Chattopadhyay, A. Hemp fiber surface modification: Its effect on mechanical and tribological properties of hemp fiber reinforced epoxy composites. *Polymer Composites* **42**, 5223–5236 (2021).
71. Svensson, B. A., Holmgren, S.-E., Gradin, P. A. & Höglund, H. High Strain Rate Compression and Sliding Friction of Wood under Refining Conditions. in 983–994 (2007).
72. Goettler, L. A., Sezna, J. & DiMauro, P. J. SHORT FIBER REINFORCEMENT OF EXTRUDED RUBBER PROFILES. *Rubber World* **187**, (1982).
73. George, J., Janardhan, R., Anand, J. S., Bhagawan, S. S. & Thomas, S. Melt rheological behaviour of short pineapple fibre reinforced low density polyethylene composites. *Polymer* **37**, 5421–5431 (1996).
74. Rowe, R. C., Sheskey, P. J. & Quinn, M. E. *Handbook of pharmaceutical excipients*. (Pharmaceutical press, 2009).
75. Roblot-Treupel, L. & Puisieux, F. Distribution of magnesium stearate on the surface of lubricated particles. *International Journal of Pharmaceutics* **31**, 131–136 (1986).
76. Hosseini, S., Venkatesh, A., Boldizar, A. & Westman, G. Molybdenum disulphide—A traditional external lubricant that shows interesting interphase properties in pulp-based composites. *Polymer Composites.* **42**, 4884–4896 (2021).
77. Forming handsheets for physical tests of pulp, Test Method TAPPI/ANSI T 205 sp-18. (2006).

78. Charles M., H. *Hansen Solubility Parameters: A User's Handbook, Second Edition*. (CRC Press, 2007).
79. Van Krevelen, D. W. & Te Nijenhuis, K. Chapter 7 - Cohesive Properties and Solubility. in *Properties of Polymers (Fourth Edition)* (eds. Van Krevelen, D. W. & Te Nijenhuis, K.) 189–227 (Elsevier, 2009).
80. Hiorns, R. Polymer Handbook, 4th edn, Edited by J Brandup, EH Immergut and EA Grulke, Associate Editors A Abe and DR Bloch, John Wiley and Sons, New York. *Polymer International* **49**, 807–807 (2000).
81. Arminger, B., Gindl-Altmutter, W., Keckes, J. & Hansmann, C. Facile preparation of superhydrophobic wood surfaces via spraying of aqueous alkyl ketene dimer dispersions. *RSC Adv.* **9**, 24357–24367 (2019).
82. Onda, T., Shibuichi, S., Satoh, N. & Tsujii, K. Super-Water-Repellent Fractal Surfaces. *Langmuir* **12**, 2125–2127 (1996).
83. Seppänen, R., von Bahr, M., Tiberg, F. & Zhmud, B. Surface energy characterization of AKD-sized papers. *Journal of Pulp and Paper Science (JPPS)* **30**, 70–73 (2004).
84. Gårdebjer, S. *et al.* Using Hansen solubility parameters to predict the dispersion of nano-particles in polymeric films. *Polym. Chem.* **7**, 1756–1764 (2016).
85. Hansen, C. M. Chapter 18. in *Hansen Solubility Parameters A User's Handbook* 321–344 (CRC Press, 2007).
86. Hristov, V. & Vlachopoulos, J. Effects of polymer molecular weight and filler particle size on flow behavior of wood polymer composites. *Polymer Composites* **29**, 831–839 (2008).
87. Ariffin, A., Ariff, Z. M. & Jikan, S. S. Evaluation on extrudate swell and melt fracture of polypropylene/kaolin composites at high shear stress. *Journal of Reinforced Plastics and Composites* **30**, 609–619 (2011).

88. Ashori, A. Wood–plastic composites as promising green-composites for automotive industries! *Bioresource Technology* **99**, 4661–4667 (2008).

89. Forsgren, L. Processing and properties of thermoplastic composites containing cellulose nanocrystals or wood-based cellulose fibres, PhD thesis. (Chalmers University of Technology, 2020).

90. Baiardo, M., Frisoni, G., Scandola, M. & Licciardello, A. Surface chemical modification of natural cellulose fibers. *Journal of Applied Polymer Science* **83**, 38–45 (2002).

91. Vandi, L.-J. *et al.* Extrusion of wood fibre reinforced poly(hydroxybutyrate-co-hydroxyvalerate) (PHBV) biocomposites: Statistical analysis of the effect of processing conditions on mechanical performance. *Polymer Degradation and Stability* **159**, 1–14 (2019).

92. Schirp, A., Mannheim, M. & Plinke, B. Influence of refiner fibre quality and fibre modification treatments on properties of injection-moulded beech wood-plastic composites. *Compos. Pt. A-Appl. Sci. Manuf.* **61**, 245–257 (2014).

93. Solala, I., Koistinen, A., Siljander, S., Vuorinen, J. & Vuorinen, T. Composites of High-Temperature Thermomechanical Pulps and Polylactic Acid. *BioResources* **11**, 1125–1140 (2016).

94. Yam, K. L., Gogoi, B. K., Lai, C. C. & Selke, S. E. Composites from compounding wood fibers with recycled high density polyethylene. *Polymer Engineering & Science* **30**, 693–699 (1990).

95. Forsgren, L. *et al.* Composites with surface-grafted cellulose nanocrystals (CNC). *Journal of Materials Science* **54**, 3009–3022 (2019).

96. Kubát, J., Rigdahl, M. & Welander, M. Characterization of interfacial interactions in high density polyethylene filled with glass spheres using dynamic-mechanical analysis. *Journal of Applied Polymer Science* **39**, 1527–1539 (1990).

97. Soucy, J., Godard, F., Rivard, P. & Koubaa, A. Rheological behavior of high-density polyethylene (HDPE) filled with paper mill sludge. *Journal of Applied Polymer Science* **135**, 46484 (2018).

98. Hristov, V., Takács, E. & Vlachopoulos, J. Surface tearing and wall slip phenomena in extrusion of highly filled HDPE/wood flour composites. *Polymer Engineering & Science* **46**, 1204–1214 (2006).

99. Adhikary, K. B., Park, C. B., Islam, M. R. & Rizvi, G. M. Effects of Lubricant Content on Extrusion Processing and Mechanical Properties of Wood Flour-High-density Polyethylene Composites. *Journal of Thermoplastic Composite Materials* **24**, 155–171 (2011).

100. Mazzanti, V. & Mollica, F. A Review of Wood Polymer Composites Rheology and Its Implications for Processing. *Polymers* **12**, 2304 (2020).

101. Irvine, G. M. The significance of the glass transition of lignin in thermomechanical pulping. *Wood Sci. Technol.* **19**, 139–149 (1985).

102. Salmen, L. TEMPERATURE AND WATER INDUCED SOFTENING BEHAVIOUR OF WOOD FIBER BASED MATERIALS, PhD thesis. (1982).

103. Guan, N., Thunell, B. & Lyth, K. On the friction between steel and some common swedish wood species. *Holz als Roh-und Werkstoff* **41**, 55–60 (1983).